4-1999

Gas Sparging and Humic Acid Sorption/Desorption

Masaki Sakakibara
Western Michigan University

Recommended Citation

Sakakibara, Masaki, "Gas Sparging and Humic Acid Sorption/Desorption" (1999). *Masters Theses*. 4347.
https://scholarworks.wmich.edu/masters_theses/4347

GAS SPARGING AND HUMIC ACID SORPTION/DESORPTION

by

Masaki Sakakibara

A Thesis
Submitted to the
Faculty of The Graduate College
in partial fulfillment of the
requirements for the
Degree of Master of Arts
Department of Chemistry

Western Michigan University
Kalamazoo, Michigan
April 1999

ACKNOWLEDGMENTS

I would like to express my deepest appreciation and gratitude to my advisor Dr. Susan Burns, for her financial support and guidance throughout this research. I am also very grateful to my committee members, Dr. Jay Means, Dr. John Chateauneuf and Dr. Donald Schreiber for their time, advice, assistance, and the critical review of this manuscript. Without their help, I would not have come this far.

Finally I would like to acknowledge my family and friends for their constant support and without whom my success would not have been possible. Especially my patient wife Kumi Sakakibara who was always there for me with encouragement and support during the course of my degree. I would never have been able to accomplish this degree without her support and encouragement.

Masaki Sakakibara

GAS SPARGING AND HUMIC ACID SORPTION/DESORPTION

Masaki Sakakibara, M.A.

Western Michigan University, 1999

Partition coefficients (K_{DOC}) for sorption of PAHs and chlorinated benzenes to dissolved humic acids (HA) were measured using gas-sparging methodology. The resulting K_{DOC} values were significantly lower than the K_{ow}-based K_{DOC} values, which generally appear to provide reliable estimates for K_{DOC} values. The K_{DOC} values measured by gas sparging were also strongly influenced by the concentration of HA in solution, as measured by dissolved organic carbon content (DOC). Increasing DOC concentration consistently resulted in decreased K_{DOC} values for all compounds investigated. Previous studies have claimed that K_{DOC} values measured using gas sparging are most accurate at high DOC concentrations, even though the resulting reported K_{DOC} values are significantly lower than K_{ow}-based K_{DOC} values. In the current work, linear regressions of K_{DOC} vs DOC concentration showed that K_{DOC} values measured at lower DOC concentrations better agreed with K_{ow}-based K_{DOC} values. Additionally, this DOC-concentration-dependent phenomena was simulated using the new idea of solute exchange between DOC and gas phases, based on the observations that DOC does accumulate at air-water interfaces.

TABLE OF CONTENTS

ACKNOWLEDGMENTS ii

LIST OF TABLES v

LIST OF FIGURES vi

CHAPTER

I. INTRODUCTION 1

- Structure and Properties of HS 1
- The Role of HS in Environment 3
- Association of HOCs With HS 5
- Kinetics of Association 11
- Problem Statement 16

II. EXPERIMENTAL SECTION 17

- Materials 17
- Analysis 17
- Curve Fitting 18
- Preparation of Humic Acid Solutions 18
- Gas Sparging Experiments 19

III. RESULTS AND DISCUSSION 22

- Multi-Compartment Model 22
  - Theory of Multi-Compartment Model 22
  - Results Obtained From Multi-Compartment Model 24
  - Expected Results From Multi-Compartment Model 29

Table of Contents—continued

CHAPTER

Effect of DOC on K_{DOC} Values 34

K_{DOC} From Apparent Henry's Law 35

Apparent Henry's Law 35

Chlorinated Benzenes 38

Comparison With Other Work 42

K_{DOC}' vs DOC Concentration Linear Regression Analysis 44

Gas Sparging and K_{DOC} 49

Mass Transfer Between Solution and Gas Phases 49

Mass Transfer Between HA and Gas Phases 53

IV. CONCLUSIONS 58

REFERENCES 61

APPENDICES

A. Raw Data 66

BIBLIOGRAPHY 72

LIST OF TABLES

1. Poisson Distribution for Solutes in HA at [DOC]=1 mg/L............................ 13
2. K_{DOC} Values From Multi-Compartment Model.. 28
3. Chlorinated Benzenes Regression-Based K_{DOC}' and K_{ow}-Based K_{DOC} Values 48

LIST OF FIGURES

1. Structural Units in Lignin and Cellulose 1
2. Poisson Distribution for Solutes in HA Solution at [DOC]=1 mg/L 14
3. DOC and Solute Concentration Effects on the Distribution of QCB in HA Solution 15
4. Gas Sparging Experimental System Configuration 20
5. Multi-Compartment Model for Gas Sparging of HA Solutions 22
6. Rate Plot for Change in Naphthalene Concentration Relative to Initial Value in HA and Water Solutions 25
7. Rate Plot for Change in 2,6-Dimethylnaphthalene Concentration Relative to Initial Value in HA and Water Solutions 26
8. Rate Plot for Change in QCB Concentration Relative to Initial Value in HA and Water Solutions 27
9. Rate Plot for Volatilization of Naphthalene out of Aqueous and HA Solutions 29
10. Expected Curves for Naphthalene Volatilization From HA Solution Given Fixed k_s (ks=1.7 x 10^2) 33
11. DOC Concentration Effect on HCB K_{DOC} Values 34
12. Comparison of Curve-Fitting Approaches to HCB Time Series Data 38
13. Change in HCB K_{DOC}' With DOC Concentration 39
14. Change in QCB K_{DOC}' With DOC Concentration 40
15. Change in TeCB K_{DOC}' With DOC Concentration 40
16. Change in TCB K_{DOC}' With DOC Concentration 41
17. Change in DCB K_{DOC}' With DOC Concentration 41

List of Figures—continued

18. Rate Plot for Change in TCB Concentration Relative to Initial Value in HA and Water Solutions 42

19. Linear Regression of HCB K_{DOC}' vs DOC Concentration 45

20. Linear Regression of QCB K_{DOC}' vs DOC Concentration 46

21. Linear Regression of TeCB K_{DOC}' vs DOC Concentration 46

22. Linear Regression of TCB K_{DOC}' vs DOC Concentration 47

23. Linear Regression of DCB K_{DOC}' vs DOC Concentration 47

24. Correlation Between Chlorinated Benzene K_{ow}-Based K_{DOC} and Regression-Based K_{DOC}' Values Estimated by Linear Regression 48

25. Mass Transfer of Solute Between Aqueous Solution and Gas Phase 49

26. Mass Transfer of Solute Between HA Solution and Gas Phase 52

27. Mass Transfer of Solute Between HA Solution and Gas Phase Based on HA Accumulation at the Air-Water Interface 54

28. Predicted and Observed Effect of DOC on HCB K_{DOC}' Values 56

29. Predicted Effect of Gas Bubble Size on K_{DOC}' Values 57

30. Observed Effect of Gas Bubble Size on QCB K_{DOC}' Values 58

CHAPTER I

INTRODUCTION

Structure and Properties of HS

Humic substances (HS) are comprised of natural organic macromolecules originating in soils, peats, lignites and brown coals (c.f., 1, 2). HS are thought to be formed in-situ during the bacterial and chemical degradation of terrestrial plant litter [1] and are thought to be derived from those plant materials, such as lignin and cellulose (Figure 1) that are most resistant to degradation [4].

The macromolecules that make up HS occur as a distribution of molecules with molecular weights ranging from a few hundred to several hundred thousand daltons [5]. A variety of methods have been employed to investigate the predominant structures in humic molecules, including oxidation [6, 7], reduction [8] and pyrolysis [9, 10], as well as non-degradative methods such as ^{1}H-NMR (c.f., [11]), ^{13}C-NMR (c.f., [12, 13]) and infrared spectroscopy [14]. In terms of atomic composition, humic materials appear to be, on a mass basis, typically ~50 % carbon [1, 15], 30-50% oxygen, 4-5% hydrogen, 1-4% nitrogen and 1-2% sulfur [5, 16]. ^{13}C-NMR data suggests that about 50 % of humic carbon is aromatic, and about 50 % is aliphatic [17]. Other ^{13}C-NMR data shows that 45 % of humic carbon is aromatic, and 55 % is aliphatic [18]. Among functional groups, carbohydrate, carboxylic, ketoic, phenolic and O-C-O are 44, 33, 14, 7 and 2% respectively [18].

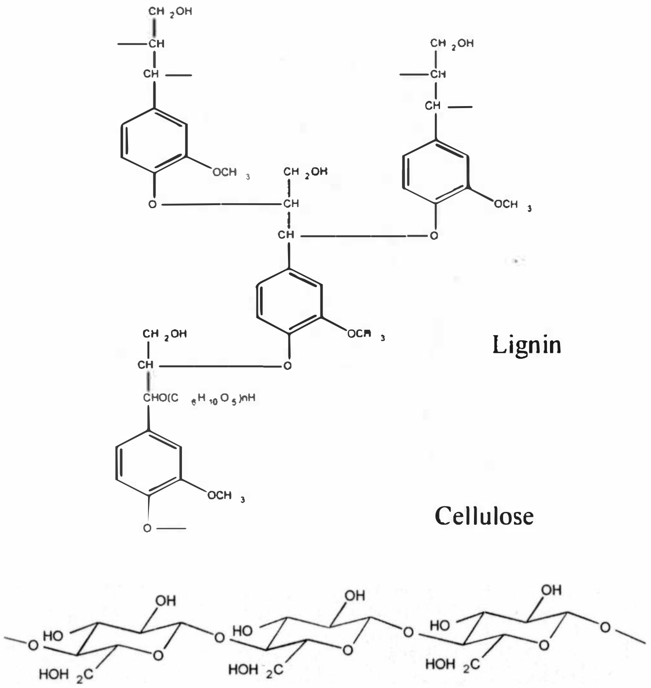

Figure 1. Structural Units in Lignin and Cellulose (Adopted from Sposito [3]).

The acid and phenolic groups in HS make humic molecules polyelectrolytic [5]. They also make some humic molecules water-soluble. Humic molecules water soluble at all pH values are defined as the fulvic acid (FA) fraction of HS. Molecules insoluble at all pH values are defined as the humin fraction of HS, and molecules insoluble at pH<2, but soluble at high pH, are defined as the humic acid (HA) fraction [19]. The molecular weight distribution of FA molecules is thought to be 100-1,000 daltons [5]. The molecular weight distribution of HA molecules is thought to be 1,000-100,000 daltons [5]. Elemental composition analysis suggests that HA and humin contain ~50% carbon by weight, while then FA is ~40% carbon by weight

[20]. FA, HA and humin average 3.5, 3.9 and 4.3% (w/w) hydrogen respectively, and 56, 35 and 42% (w/w) oxygen respectively. HA molecules therefore have the smallest H/C and O/C ratios among HS fractions. The structures of HA molecules, reflecting these differences, seem somewhat less aliphatic and more aromatic than FA, while FA is richer in carboxylic acid, phenolic, and ketonic groups [5].

The water-soluble fractions of HS are ubiquitous in fresh surface waters [19]. HS also occurs in the sediments of lakes and rivers [19]. In all three locations - soils, sediments and surface water - HS contribute significantly to the fate of transport of organic pollutants and metals [19, 21].

The Role of HS in Environment

Metals and both polar and nonpolar organic compounds are known to associate with HS in soils, sediments and water [22]. This association affects chemical, biological and photochemical transformations of compounds, as well as compound transport, accumulation and volatilization [16]. Modes of association with HS appear to include ionic bonding [23], hydrogen bonding [24], covalent bonding [25] and van der waals bonding [26]. For example, Senesi and Testini [23] used IR to look at the modes of association between HS and nitrogenated herbicides such as prometone (2-methoxy-4,6-bis(isopropylamino)s-triazine and monuron (3-(p-Chlorophenyl)-1,1-dimethylurea). HS IR absorption bands characteristic of carboxyl and carbonyl bonds were found to be strongly reduced after association of the nitrogenated herbicides with the HS, while absorption bands characteristic of ionized carboxylic and phenolic hydroxyl groups were much more intense. Based on these results, Senesi and Testini concluded that ionic bonding was occurring between the deprotonated carboxylic acid groups of the HS and the protonated N-H groups of the nitrogenated herbicides. Maqueda et al. [27] obtained similar results using a cationic organic herbicide, chlordimeform (N'-[4-chloro-2-methyl-phenyl]-N,N-dimethylmethanoimidamide). IR studies indicated that HS absorption bands characteristic of C=O were found to be reduced after association of the protonated amine group of the s-triazine with the HS. They concluded that the s-triazine associated with HS by hydrogen bonding to both HS acid functionalities and C=O [23, 24]. In other work [25], the IR N-H bands of chloroaniline were found to disappear in the presence of HS. Based on the reaction of amines with carbony groups according to

$$ArNH_2 + O{=}CR_2 \rightleftharpoons ArN{=}CR_2 + H_2O \qquad (1)$$

covalent bonding between chloroaniline and HS of aromatic carbonyl sites was suggested as being responsible for the disappearance of the IR N-H bands.

An additional mode of association with HS occurs for nonpolar hydrophobic organic compounds (HOCs) and is thought not to involve specific functional groups in HS [26]. Environmentally relevant HOCs include polychlorinated biphenyls (PCBs), polycyclic aromatic hydrocarbons (PAHs), chlorinated benzenes (Cl-Bzs) and pesticides such as DDT. The association of HOC with HS appears to decrease the bioavailability of HOCs to aquatic organisms (c.f., [28]), decrease the rate of alkaline hydrolysis of HOCs (c.f., [16]), and decrease the apparent volatilization rate of HOC from natural waters to atmosphere (c.f., [29]). As a consequence, the mode of association of HOCs with HS has received a great deal of attention.

Association of HOCs With HS

The association of HOCs with HS has been extensively investigated. Wolcott et al. [30], for example, used batch equilibrium experiments to assess the association between dissolved DDT and HS in soil. In their experiments, aqueous suspensions of soils were mixed with DDT for a predefined period and then centrifuged. HS-associated DDT concentrations were measured via the mass of DDT in the centrifuged soils. Dissolved phase (not HS-associated) DDT was defined as the difference between the soil-associated and initial DDT mass amendment. The result was a linear isoplot relating the HS-associated (or "bound", X_b) and dissolved phase (X_w) masses of DDT such that a distribution coefficient, K_d, could be defined for the process as

$$K_d = \frac{X_b/M}{X_w/V} \tag{2}$$

where V is the total aqueous volume (mL), and M is the soil mass (g). The value of K_d for DDT was $10^{5.0}$ in Houghton muck samples, meaning that HS-associated DDT per unit mass of soil (kg) occurred in 10^5-fold excess over that in the dissolved phase (per unit volume, L).

In similar work, Carter and Suffett [31] used equilibrium dialysis techniques to separately measure the associated and non-associated DDT concentrations in aqueous solutions of HA from three different sources, including the commercially available Aldrich HA. The result was a linear isoplot relating C_b and C_w to the DDT solubility limit and, based on this isoplot, Carter and Suffett proposed that HOC association with dissolved HS could be described using a partition coefficient, K_{DOC}, such that

$$K_{DOC} = \frac{C_b}{C_w[DOC]} \qquad (3)$$

where C_b (mol/L) and C_w (mol/L) are defined as the associated ("bound") and non-associated DDT concentrations, and [DOC] is the dissolved organic carbon content of the HS solution (kg/L DOC). Similar to Wolcot et al. [30], the K_{DOC} value for DDT was found to be $10^{5.4}$, indicating a $10^{5.4}$ fold excess of HS-associated DDT (per unit mass, kg) over dissolved phase DDT (per unit volume, L).

Using equilibrium dialysis techniques similar to those used by Carter and Suffett [31], Chiou et al. [32] found that the apparent solubility of HOCs such as DDT and PCBs increased with increasing concentrations of dissolved HS. As with previous work, C_b was related to C_w via a linear isoplot. Based on this isoplot, Chiou et al. [32] defined the parameter, S_w*, to describe the apparent solubility of HOCs in aqueous solutions of HS such as

$$S_w^* = S_w + XC_0 \qquad (4)$$

where X (g/mL) is the concentration of dissolved HS, S_w (μg/mL) is the HOC solubility limit in aqueous solutions without HS, and C_0 is the mass of HS-associated HOC per unit mass of dissolved organic matter (DOM) in units of μg/g. A mass-based partition coefficient, K_{DOM}, was therefore defined as

$$K_{DOM} = \frac{C_0}{S_w} \tag{5}$$

with K_{DOM} having units of mL/g. Substituting Equation 4 into Equation 5 and rearranging yields

$$K_{DOM} = \frac{S_w^* - S_w}{S_w X} \tag{6}$$

where the HS-associated concentration is represented by $(S_w^* - S_w)/X$, which equals C_0 in Equation 5. Alternatively, if X and C_0 in Equation 4 are expressed in terms of the more easily measured dissolved organic carbon (DOC) content of the HS solution, Equation 6 becomes

$$K_{DOC} = \frac{S_w^* - S_w}{S_w X} \tag{7}$$

where K_{DOC} is the HS-partition coefficient normalized to DOC concentration (L/mg DOC), as introduced by Carter and Suffett [31]. One result of Chiou's work was the discovery that K_{DOC} was related to the aqueous solubilities of HOCs, with higher solubility HOCs having lower K_{DOC} values. For example, relative to DDT, which has an aqueous solubility of 1.41 x 10^{-8} mol/L and K_{DOC} value of $10^{5.9}$ [21], naphthalene has an aqueous solubility of 2.45 x 10^{-4} mol/L and K_{DOC} value of $10^{2.9}$ [21].

Assuming HOC association with HS to be a partitioning phenomenon, Chiou [32] redefined K_{DOM} in terms of the ratio of equilibrium concentrations of HOCs in water and DOM phases:

$$K_{DOM} = \frac{C_b}{C_w[DOM]} \tag{8}$$

where C_b (mol/L) and C_w (mol/L) are the HS-associated and dissolved phase HOC concentration respectively.

Thermodynamically, a partitioning phenomenon is described by the chemical potential (μ) of solute in two different phases. For example, at equilibrium, the chemical potentials of solute in aqueous (μ_w) and HS (μ_{HS}) phases are equal such that

$$\mu_w = \mu_{HS} \tag{9}$$

Given the same reference state and standard state (i.e., pure subcooled liquid solute) each chemical potential can be represented by

$$\frac{x_{HS}}{x_w} = \frac{\gamma_w}{\gamma_{HS}} \tag{10}$$

where γ_w and γ_{HS} are the activity coefficients of the solute in water and HS phases, respectively, and x_w and x_{HS} are the respective mole fractions of the solute in the water and HS phases. Relating x_w and x_{HS} to molar concentrations yields

$$X_{HS} = C_{HS}V_{HS} \tag{11}$$

and

$$x_w = C_wV_w \tag{12}$$

where C_{HS} (mole solute in HS phase/L HS) and C_w (mole solute in water phase/L Water) are the concentrations of HS-associated and dissolved phase HOC, respectively, and V_{HS} and V_w (L/mole) are the molar volumes of HS and water respectively. Combining Equations 10-12 with Equation 8 therefore yields

$$K_{DOM} = \frac{C_{HS}}{C_w\varrho} = \frac{\gamma_w V_w}{\gamma_{HS}V_{HS}\varrho} \tag{13}$$

where ρ is the density of HS in kg/L. Defining the weight fraction of organic carbon in HS as fc, K_{DOM} can be re-expressed as K_{DOC} such that

$$K_{DOM} = K_{DOC}\,fc \tag{14}$$

and Equation 13 therefore becomes

$$K_{DOC} = \frac{\gamma_w V_w}{\gamma_{HS}V_{HS}\varrho\, fc} \tag{15}$$

Chiou et al. [33] proposed that, since aqueous solubility (S) can be represented by

$$S = \frac{1}{\gamma_w V_w} \tag{16}$$

K_{DOC} can be defined in terms of HOC solubility as

$$K_{DOC} = \frac{1}{S\gamma_{HS} V_{HS} \bullet fc} \qquad (17)$$

Equation 17 predicts that a plot of log K_{DOC} vs log S should be linear, if HOC association with HS is a partitioning phenomenon. Based on results obtained with 12 HOCs, Chiou et al. [34] concluded that log K_{DOC} was linearly related to log S and, therefore that HOC association with HS was a partitioning phenomena. Additionally, based on the slope of the line, Chiou et al. concluded that aqueous solubility was the primary HOC characteristic defining K_{DOC}.

One of the other first theoretical investigations of the associations of HOCs with HS was published by Karichoff [35] based on the behavior of HS in soils and sediments. Similar to Chiou, Karickhoff defined a partition coefficient, K_{DOC}, that was based on the organic carbon content of the HS. Karickoff [35] proposed that K_{DOC} should be related to other water-organic partition coefficients if HOC association was a partitioning phenomenon. Using K_{ow}, the octanol-water partition coefficient. Karickhoff found that K_{DOC} values for 47 HOCs could be related to K_{ow} by

$$K_{DOC} = 0.411 K_{OW} \qquad (18)$$

K_{ow} can be represented by

$$K_{OW}=\frac{C_o}{C_w}=\frac{\gamma_w V_w}{\gamma_o V_o} \tag{19}$$

where γ_w and γ_o are activity coefficients of solute in water and organic phases respectively. Substituting Equation 19 into 15 gives

$$K_{DOC}=K_{OW}\frac{\gamma_o}{\gamma_{HS}\varrho\ fc}\left(\frac{V_o}{V_{HS}}\right) \tag{20}$$

where the proportionality constant in Equation 18 (i.e., 0.411) is those terms in Equation 20 to the right of K_{ow}. As with Chiou's work [33], this work indicated that HOC association with HS depends largely on aqueous solubility. The relative magnitudes of the contributions of γ_w and γ_{HS} to K_{DOC} is exemplified by naphthalene, whose γ_w and γ_{HS} are $10^{11.1}$ and $10^{2.9}$ [36] respectively. Respective values for ρ and fc are 0.67 mL/g [37] and 0.502 [38].

Kinetics of Association

Chiou et al. [32, 33] and Karickoff et al. [35] speculated that the association of HOCs with HS could be explained by employing the idea of partitioning behavior. However, the association between HOCs and HS cannot reach equilibrium. This is because the HS phase is distributed in water as a discontinuous phase. Equilibrium, under these conditions, would require the chemical potential of a HOC to be the same in all HS molecules. Even assuming that HS occurred as a single macromolecule, rather than as a distribution, equilibrium-like conditions would only exist at HS occupancies of ≥ 9, meaning that each HS molecule would have to be associated with ≥ 9 HOC molecules [39]. This requirement for a minimum occupancy number is based on molecules being distributed in HS molecules according to a Poisson distribution [40], as is found for the distribution of molecules in micelles [39, 41]. A Poisson distribution differs from a normal distributions in that it is discrete, not continuous. According to the Poisson distribution, HOC molecules occur associated with HS molecules as integers: an HS molecule may contain only 0, 1, 2,...n HOC molecules, although the average number, N, need not be an integer.

Table 1 lists values of N per 10^{-6} kg/L DOC and probabilities for actual occupancy number, n, for a series of HOCs. Values of N were calculated from [40]

$$N = 10^{-3} fcMW_{HA} \frac{K_{DOC}}{1 + K_{DOC}[DOC]} C_w^{SAT} \tag{21}$$

where the C_w^{SAT} and MW_{HA} are the solubility of solute in water at saturation and molecular weight of HA. Assuming MW_{HA} is 50,000 g/mol, probabilities for occupancy number, Pr_n, were calculated from

$$Pr_n = e^{-N} \frac{N^n}{n!} \tag{22}$$

Fuller distributions corresponding to Table 1 are shown graphically in Figure 2. Note that the values in Table 1 are maxima, and that N will decrease both with increasing DOC concentration and with decreasing HOC concentration. In the case of pentachlorobenzene (QCB), for example, increasing DOC concentration to 50 mg/L

Table 1

Poisson Distribution for Solutes in HA at [DOC]=1 mg/L

Compound	K_{DOC} *	N	Closest n	Pr_n	Pr_{n+1}	Pr_{n-1}
Hexachlorobenzene (HCB)	$10^{5.50}$	4.65	5	0.19	0.13	0.18
Pentachlorobenzene (QCB)	$10^{3.61}$	11.17	11	0.12	0.11	0.12
Phenanthlene	$10^{4.18}$	12.93	12	0.11	0.11	0.10
Biphenyl	$10^{3.51}$	10.68	11	0.12	0.11	0.12

* K_{DOC} values from refs 21 and 35.

changes N to 3.81, while changing the concentration of QCB to one third C_w^{SAT} changes N to 3.72. The effect of these changes on Pr_n is illustrated in Figure 3.

Equilibrium distribution of an HOC between water and HS phases is consequently impossible, since it would require equivalence in the chemical potentials of the HOC in water and all HOC molecules. The apparent constant distribution of HOC between water and HS molecules must therefore be the result of steady-state kinetics.

Hassett and Milicic [29] were the first to incorporate steady-state kinetics into the description of K_{DOC}. In this description, association of HOCs with HS occurs via

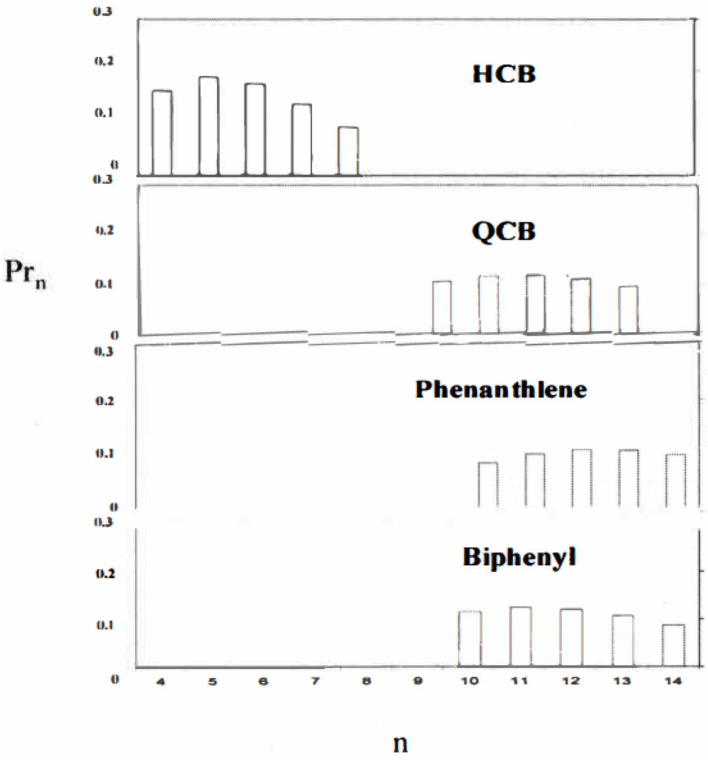

Figure 2. Poisson Distribution for Solutes in HA Solution at [DOC]=1 mg/L.

bimolecular encounter between HOC and HS such that

$$\mathrm{HOC} + \mathrm{HS} \xrightarrow{k_s} \mathrm{HOC} - \mathrm{HS} \tag{23}$$

where this forward process, called sorption, is a second-order rate process having a second-order rate constant (k_s) with units of t^{-1} (kg/L DOC)$^{-1}$. Dissociation is similarly represented by

$$\mathrm{HOC} - \mathrm{HS} \xrightarrow{k_d} \mathrm{HOC} + \mathrm{HS} \tag{24}$$

This process, called desorption, is a first-order process having a first-order rate

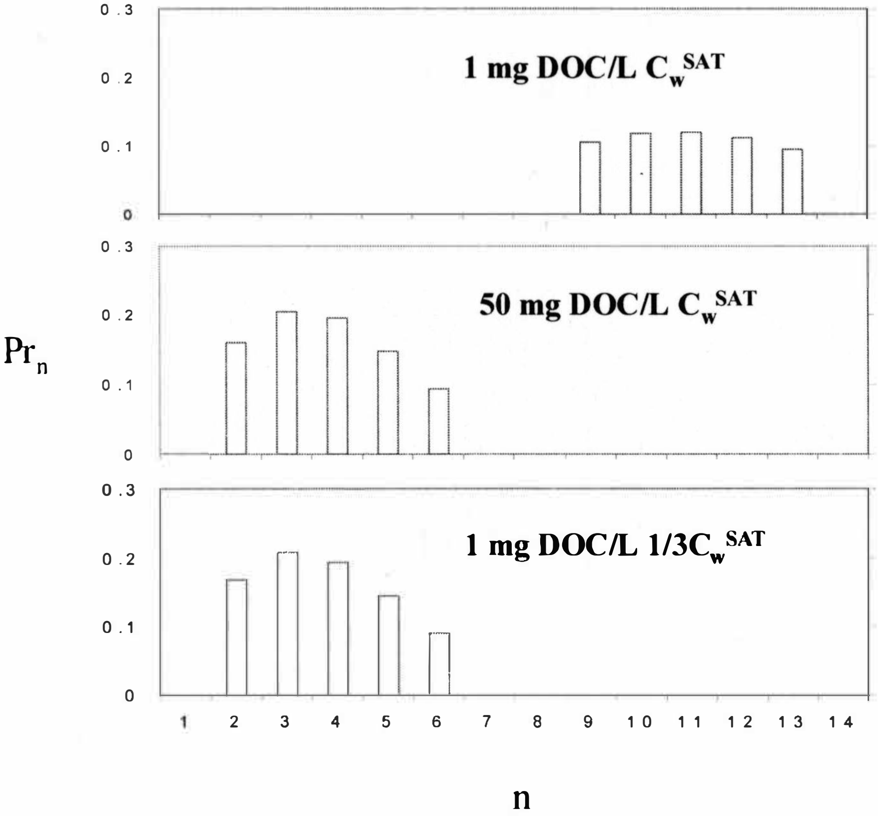

Figure 3. DOC and Solute Concentration Effects on the Distribution of QCB in HA Solution.

constant with units of t^{-1}. Based on these processes, K_{DOC} becomes

$$K_{DOC} = \frac{k_s}{k_d} \tag{25}$$

Milicic and Hassett [29] tested the equivalence of Equations 25 and 3 using techniques based on gas sparging. The results were k_s and k_d values for PCB 52 of 1.7

x 10^2 min^{-1} (kg/L DOC)$^{-1}$ and 3.5 x 10^{-3} min^{-1} respectively, for a K_{DOC} of 7.1 x 10^4. The significance of kinetics in defining HOC association with HS resides in the overlap between HOC residence times in HS and the time frame for processes affecting HS-sorbed and dissolved phase (not-sorbed) HOCs. For example, HSs have been found to be photochemically active in sunlit natural waters, producing a variety of highly reactive but short-lived reactants such as HO•, e_{aq}^-, etc. (c.f. [16]). Few chemical classes are resistant to transformation by HS photochemical activity, suggesting that HS could be important to the degradation of pollutants in the aquatic environment. However, there is now evidence that access to some HS photoreactivity requires that compounds be present in HS long enough for HS photoabsorption and reactant production to occur. In terms of other processes, there is evidence that bioavailability possibly dependent on the probability of encountering compounds only during the time the compounds are not sorbed to HS.

Problem Statement

The purpose of the current work is to evaluate the ability of gas sparging methodology in measuring the kinetics of sorption to and desorption from HS for a series of compounds that span chemical class and K_{DOC} values.

CHAPTER II

EXPERIMENTAL SECTION

Materials

Humic Acid (sodium salt), 1,3,5-trichlorobenzene (99%), 1,2,4,5-tetrachlorobenzene (98%), pentachlorobenzene (99%), hexachlorobenzene (99%), biphenyl (99%), 2,3-dimethylnaphthalene (98%), 2,6-dimethylnaphthalene (98%), naphthalene (99+%), phenanthrene (98%), bibenzyl (99%) and fluorene (98%) were purchased from Aldrich Chemical Company. 2,2',5,5'-tetrachrolobiphenyl (99%), 2,3-dichlorobiphenyl (99%) and 2,2,5-trichlorobiphenyl (99%), 2,4,5,6-tetrachloro-m-xylene (99%), decachlorobiphenyl (99+%) and lindane (99%) were purchased from Ultra Scientific. Sodium chloride (certified ACS), iso-octane (Optima), hexane (Optima), acetone (Optima), methanol (HPLC), potassium phosphate (certified ACS), potassium phosphate monobasic (certified ACS), hydrochloric acid (certified ACS PLUS), and sodium hydroxide (certified ACS) were obtained from Fisher Scientific Company. Chromic acid (10% w/v) was purchased from Lab Chem Inc. All aqueous solutions were prepared using Elgastat Maxima-HPLC water (Elga Ltd). All chemicals were used without further purification unless otherwise noted.

Analysis

All quantitative measurements of HOCs were done by gas chromatography

(GC). The GC was a Hewlett Packard Series 5890 II Plus equipped with flame ionization (FID) and electron capture (ECD) detectors. The column was a 30m x 0.32mm (i.d.) capillary column coated with 5% polydiphenyldimethysiloxane (0.25 µm film thickness). Quantification was by internal standard with relative response factor determined from a standard curve. 2,4,5,6-Tetrachloro-m-xylene decachlorobiphenyl (99+%) and lindane (99%) were used as standards for chlorinated compounds. 2-Methylnaphthalene and bibenzyl were used as standards for polyaromatic hydrocarbons (PAHs).

Curve Fitting

Non-linear curve-fitting was performed using Scientist V 2.0 (MicroMath Scientific). Conditions for parameter estimations were specified when necessary to force parameter estimates to assume the appropriate sign (e.g., parameter >0). Non-linear curve-fitting was performed without weighting the data. Linear regressions were performed using Microsoft Excel 97.

Preparation of Humic Acid Solutions

Humic acid (HA) stock solutions were prepared according to the method of Zepp et al [42]. Aldrich HA, ranging from 1g through 28 g, was dissolved in 2 L of0.1 N sodium hydroxide mixed for 1 hour, and filtered under pressure (2-4 psig) through a 0.20 µm Gelman Science capsule filter (No. 12117). The filtrate pH was adjusted to pH 6 by adding HCl, filtered again, and the filtrate pH was re-adjusted to pH 6 by adding HCl and/or NaOH. Concentrations of HA stock and working solutions were determined spectroscopically using the method of Zepp [42]. HA stock solutions were stored in amber bottles at 4°C until used. Working solutions were prepared by dilution of stock solutions.

Gas Sparging Experiments

Gas purging experiments were performed using 2L, 11 x 32.5 cm heavy-walled borosilicated glass bottles (Environmental Bottle) (Figure 4). Sparging gas was introduced into bottles via 1/8" 316SS tubing inserted into a through-port in the bottle cap. The depth of gas introduction was 23 cm from the solution surface unless otherwise specified. In some experiments, a gas diffusing stone (Fisher Scientific Company No 11-139B, 60 μm pore size) was attached to the gas introduction tubing. Gas flow was monitored with rotometers (Cole-Parmer, E-32460-46 and E-32460-42).

HA and water solutions for gas sparging experiments (2L) were prepared in sparging bottles by amending the solutions with analytes dissolved in small volumes of either methanol or hexane (10-300 μl). The resulting analyte concentrations were either 1/3 the reported aqueous solubility [21] or 10^{-5} M, whichever was less [35]. After amendment, solutions in fully-assembled gas sparging apparatus (Figure 4) were stirred overnight using a stir-plate and glass-coated magnetic stirring bar. Time-series samples (7-12 samples) were taken during gas sparging experiments via a through-port in bottle caps using a glass syringe and a 316SS flat-tipped needle. Samples were transferred to culture tubes having teflon-lined caps. The syringe was thoroughly washed with 4 ml of hexane after each sample, with the wash added to each sample.

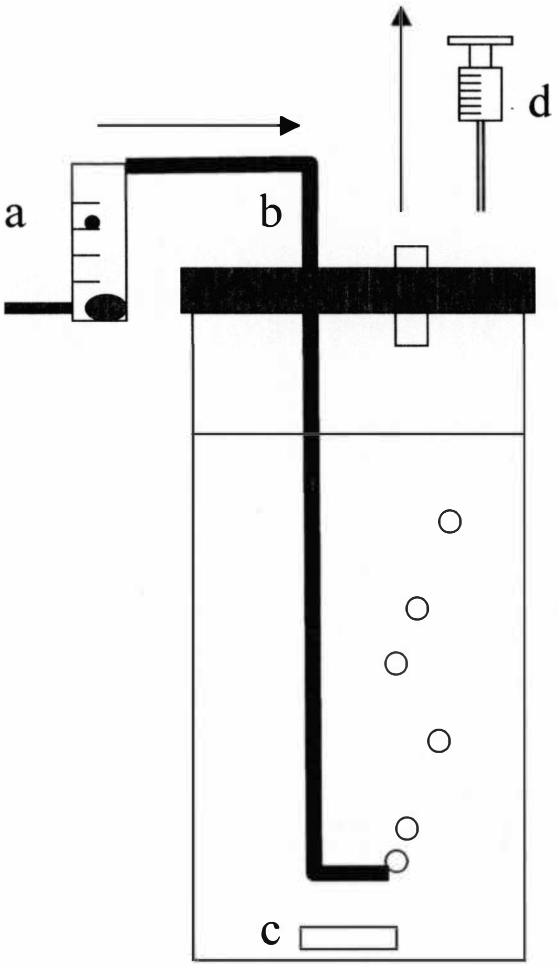

Legend. a = Flow meter with needle pressure regulator, b = Stainless steel tube (316SS), c = Glass coated magnetic stirring bar, d = Glass syringe

Figure 4. Gas Sparging Experimental System Configuration.

Total sample volumes taken during the course of experiments were less than 10% of the total solution volume. Water samples containing no HA were extracted by liquid-liquid extraction. HA solution samples were extracted using a previously described chromic acid digestion extraction technique [40, 43]. The extraction solvent used was hexane unless otherwise specified, and extracts were concentrated, if necessary, under a gentle air flow.

CHAPTER III

RESULTS AND DISCUSSION

Multi-Compartment Model

Theory of Multi-Compartment Model

Hassett and Milicic [29] used gas sparging of humic acid (HA) solutions to investigate rates of sorption to and desorption from HA. This methodology is based on the idea that only dissolved phase (not sorbed) molecules undergo volatilization during gas purging of HA solution. Gas-sparged HA solution can be represented by the multi-compartment model in Figure 5. In Figure 5, k_v (min^{-1}), k_s (L/kg DOC min^{-1}) and k_d (min^{-1}) represent rate constants for HOC volatilization, association with HS (sorption) and dissociation from HS (desorption), respectively, and C_g, C_d and C_s

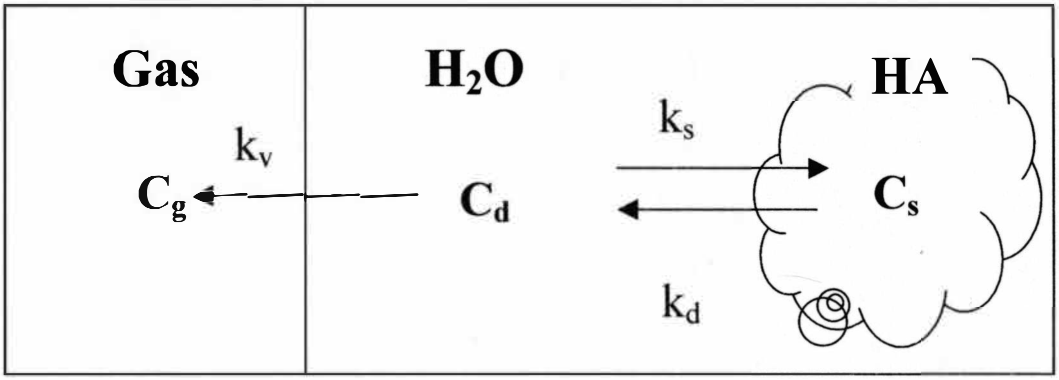

Figure 5. Multi-Compartment Model for Gas Sparging of HA Solutions.

represent the concentration of hydrophobic organic compound (HOC) in the gas, dissolved and HA phases, respectively. In the gas-sparging method, the value of k_v is measured independently in aqueous solutions containing no HA. This technique was first introduced by Mackay et al. [45] to measure Henry's law constants, and the application is based on the idea that the rate of mass transfer from liquid to gas phase is constant, and also controlled by the liquid phase [45,46]. This allows the rate constant for volatilization (k_v) to be determined given a constant solution volume, solution depth and gas flow rate. Applied to HA solution, the mass transfer gradient of solute in each phase is describable by

$$\frac{dC_s}{dt} = k_s[DOC]C_d - k_dC_s \tag{26}$$

$$\frac{dC_d}{dt} = k_dC_s - (k_v + k_s[DOC])C_d \tag{27}$$

$$\frac{dC_T}{dt} = -\frac{dC_g}{dt} = -k_vC_d \tag{28}$$

where C_T is the total solution concentration, given by

$$C_T = C_s + C_d \tag{29}$$

Given known k_v and dissolved organic carbon (DOC) concentration values, Equations 26-29 have only two unknown parameters - ks and kd. Estimates for these values can be obtained from a rate plot of the change in C_T with time during sparging. Values are determined from non-linear curve-fitting to the data. Curve-fitting is possible using the undifferentiated Equations, 26-29 if the initial conditions for C_d, C_s and C_T are specified by

$$C_s = \frac{\frac{k_s}{k_d}[DOC]}{(1+\frac{k_s}{k_d}[DOC])} \tag{30}$$

$$C_d = \frac{1}{(1+\frac{k_s}{k_d}[DOC])} \tag{31}$$

$$C_T=C_0 \tag{32}$$

where C_0 is C_T at t=0.

Results Obtained From Multi-Compartment Model

Figure 6 shows a time series plot for gas purging of naphthalene out of aqueous and HA solutions. The gas flow rate was 3 L/min, and the DOC concentration was 1710 mg/L. At this concentration, given Karickhoff's [35] method for estimation K_{DOC} from K_{ow} (Equation 18) [21], 60 % of the naphthalene in the HA solution would be expected to initially sorbed to HA (fb=0.60) [21]. The value for f_b is calculated from K_{DOC} and DOC concentration by [26]

$$f_b = \frac{K_{DOC}[DOC]}{1+K_{DOC}[DOC]} \tag{33}$$

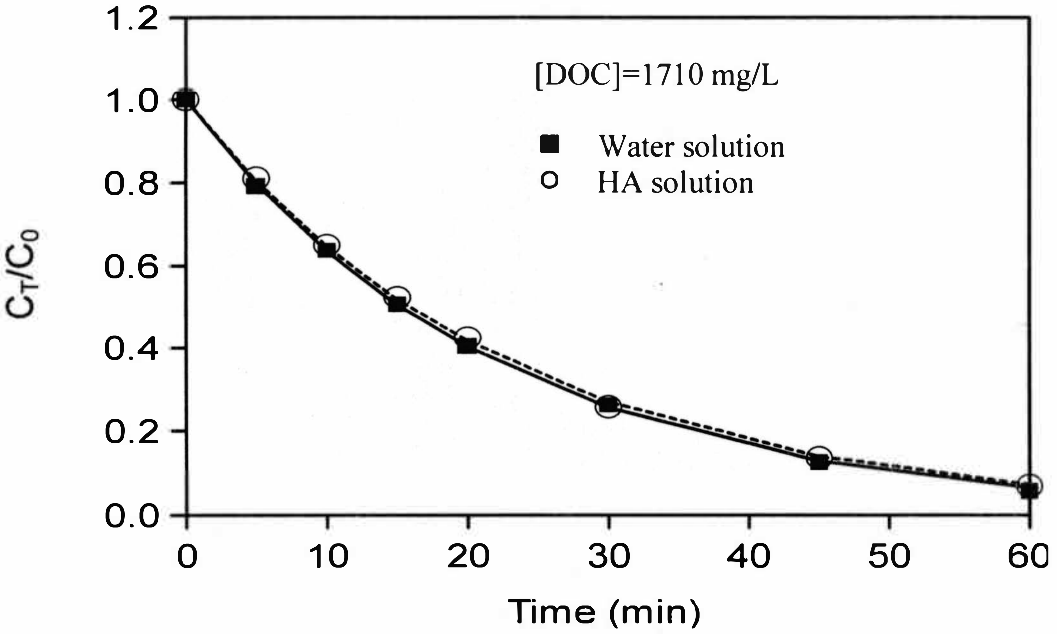

Figure 6. Rate Plot for Change in Naphthalene Concentration (C_T) Relative to Initial Value (C_0) in HA and Water Solutions.

Curve-fitting of the multi-compartment model (Equations 26-32) to the data gives values of k_s and k_d of 4.66 min^{-1} (kg DOC/L)$^{-1}$ and 0.131 min^{-1}, respectively. These values are different from the values Milicic and Hassett [29] report for 2,2',5,5'-tetrachlorobiphenyl, PCB 52, (k_s=1.7 x 10^2 L/kg DOC min^{-1} and k_d=3.5 x 10^{-3} min^{-1}). The K_{DOC} value calculated by curve-fitting of the multi-compartment model is 24, as compared to the K_{ow}-based value of 880 [21]. The experimental value is therefore nearly two orders of magnitude below the K_{ow}-based value, and suggests that the initial fb=0.30 in the HA solution.

Similar results were obtained for other compounds. Another rate plot, this time for 2,6-dimethylnapthalene, is shown in Figure 7. The gas flow rate during this experiment was the same as for naphthalene (3 L/min), and the DOC concentration was 1070 mg/L. The K_{ow}-based K_{DOC} value for 2,6-dimethylnaphthalene is 8.4 x 10^3 [21], meaning that 90 % of 2,6-dimethylnaphthalene is expected to be initially sorbed to HA in this solution. Curve-fitting Equations 26-32 to the data gives values of k_s and k_d of 180 min^{-1} (kg/L DOC)$^{-1}$ and 4.4 min^{-1} respectively. The K_{DOC} value calculated from k_s and k_d is 40. As with naphthalene, then, the experimental K_{DOC} value is nearly two orders of magnitude below K_{ow}-based value, and suggests that fb=0.04 in the initial HA solution.

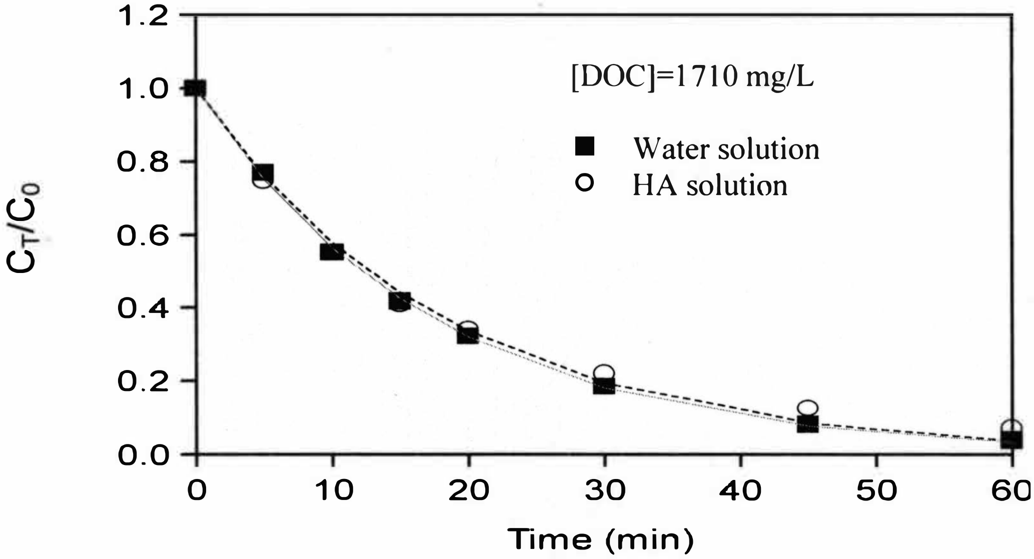

Figure 7. Rate Plot for Change in 2,6-Dimethylnaphthalene Concentration (C_T) Relative to Initial Value (C_0) in HA and Water Solutions.

Figure 8 shows a rate plot for gas purging of pentachlorobenzene (QCB) out of aqueous and HA solutions (DOC concentration of 1830 mg/L). The gas flow rate in this experiment was 2 L/min. Given K_{ow}=10^5 for QCB, fb is expected to be 0.99 in the initial HA solution. Curve-fitting of Equation 26-32 to the data gives values of

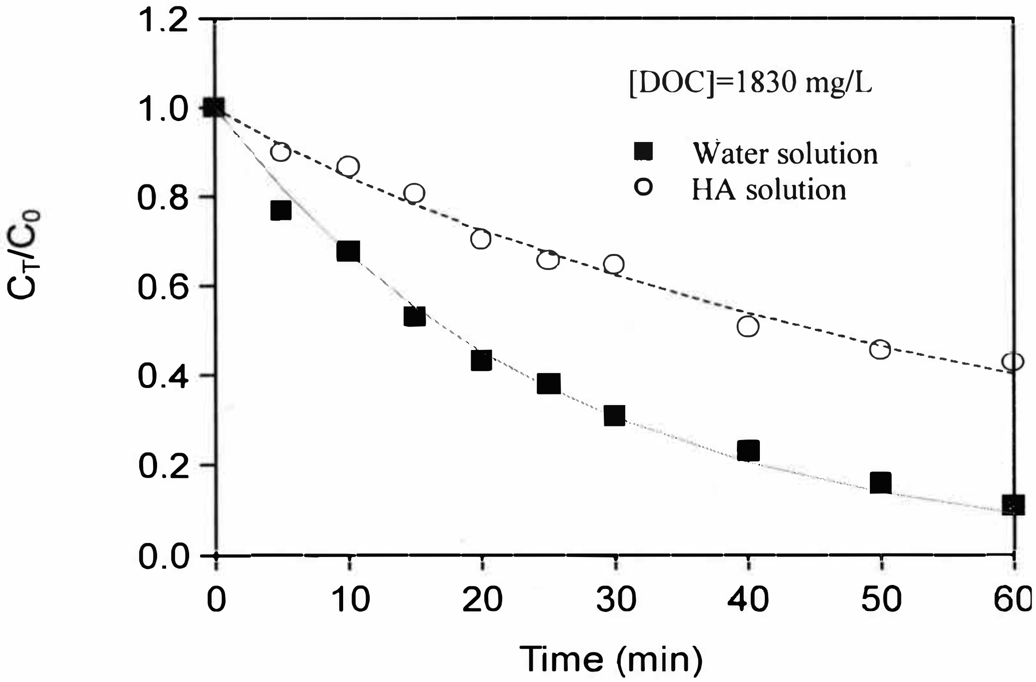

Figure 8. Rate Plot for Change in QCB Concentration (C_T) Relative to Initial Value (C_0) in HA and Water Solutions.

ks=30 min^{-1} (kg/L DOC)$^{-1}$, and k_d=0.047 min^{-1}, yielding K_{DOC}=640, as compared to the K_{ow}-based value of 4.1 x10^4 [21]. The experimental value is nearly two orders of magnitude below K_{ow}-based value, and suggests that fb=0.54 initially in the HA solution.

Values of k_s and k_d yielding unexpectedly low K_{DOC} values were measured for a variety of compounds from different chemical classes. Other K_{DOC} value determined using the multi-compartment model are listed in Table 2.

Table 2

K_{DOC} Values From Multi-Compartment Model

Compound	K_{DOC} Obtained from Multi-Compartment Model	K_{DOC} Estimated From K_{ow} *	[DOC] mg/L
Naphthalene	2.4×10^1	8.8×10^2	1710
2,6-dimethylnaphthalene	4.0×10^1	8.4×10^3	1070
2,3-dimethylnaphthalene	2.1×10^2	1.0×10^4	892
Phenanthrene	4.7×10^2	1.5×10^4	601
1,3-dichlorobenzene (DCB)	1.6×10^2	1.0×10^3	1829
1,2,4,5-tetrachlorobenzene (TeCB)	2.4×10^3	1.3×10^4	112
Pentachlorobenzene (QCB)	4.9×10^3	4.1×10^4	49
Hexachlorobenzene (HCB)	1.1×10^5	1.3×10^5	28
2,2',5,5'-tetrachlorobiphenyl (PCB52)	8.7×10^3	5.2×10^5	61
2,2',3,3',4,4'-hexachlorobiphenyl (PCB128)	8.8×10^6	4.1×10^6	5.3

* K_{ow} values from ref. 21.

Expected Results From Multi-Compartment Model

Because the sparging experiments commonly gave K_{DOC} values much lower than expected, the effect of k_s, k_d and K_{DOC} values on the experimental behavior of compounds in gas-purging experiments was investigated using computer simulations and Equations 26-32. The effect of k_s and k_d on the experimental behavior of naphthalene is shown in Figure 9. In this plot the observed behavior of naphthalene is indicated by the data points, and the line through data points is the curve-fit

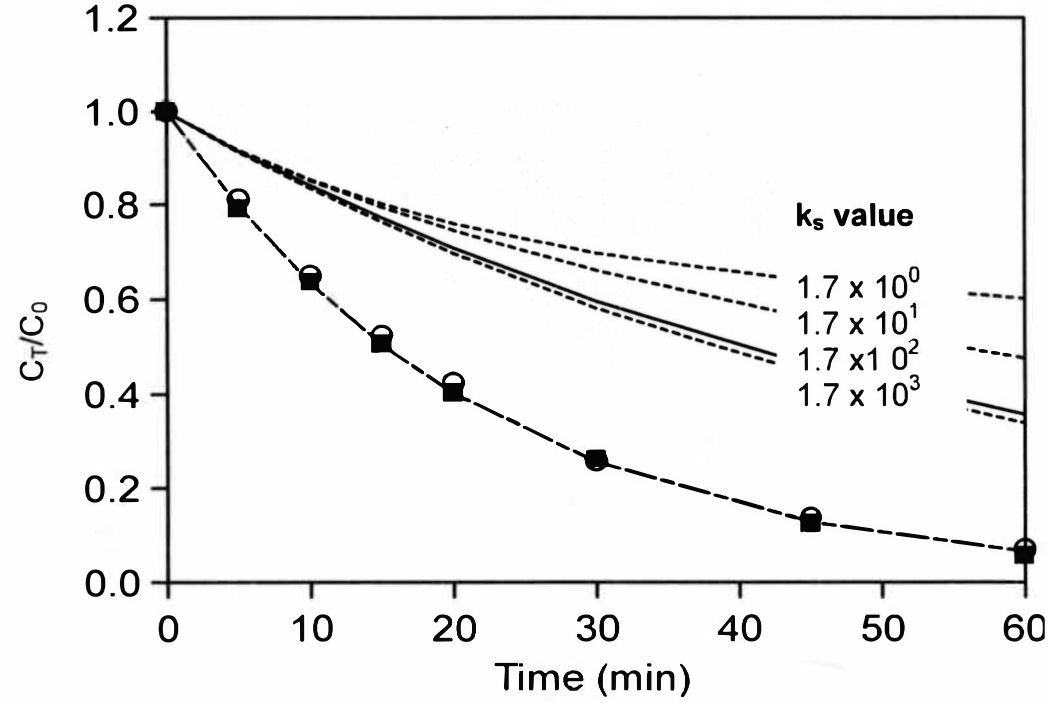

Figure 9. Rate Plot for Volatilization of Naphthalene out of Aqueous (■) and HA (O) Solutions.

yielding k_s=4.66 min^{-1} (kg /L DOC)$^{-1}$ and k_d=0.131 min^{-1}. Assuming K_{DOC}=880, as predicted from K_{ow}=1.9 x 10^3 [21], the solid line is the expected behavior in HA solution containing DOC concentration of 1710 mg/L, provided that k_s=1.7 x 10^2 min^{-1} (kg/L DOC)$^{-1}$, the value measured by Milicic and Hassett for PCB 52, and k_d=k_s/K_{DOC} [29]. As Figure 9 illustrates, given an initial fb=0.60 and values of k_s and k_d similar to those previously reported [29], the rate of volatilization of naphthalene from HA solution is expected to be significantly slowed relative to solution without HA solution. As k_s and k_d values are decreased, the volatilization rate also decreases, and as k_s and k_d values are increased, the volatilization rate increases until a limit is reached at $k_s>10^3$ min^{-1} (kg/L DOC)$^{-1}$ and $k_d>10^4$ min^{-1}.

These simulated results reflect the current understanding that HOCs sorbed to HA do not exchange directly with the gas phase, but must desorb first in order to volatilize. The limit on volatilization rate reached at high k_s and k_d values occurs at values significantly lower than those expected for diffusion-controlled exchange between sorbed and dissolved phases. Values for the diffusion controlled rate constants can be derived from basic kinetic theory, which states that any bimolecular reaction rate constant, k, can be represented by

$$k = p\,Z\,e^{-E_a/RT} \qquad (34)$$

where Z is the collisional frequency between reacting molecules at unit concentration (L/mol), E_a is the energy of activation for the reaction, R is the gas constant, T is absolute temperature and p represents the probability that factors, such as proper orientation, will be met for any collision. Z can be further defined by

$$Z = \frac{4\pi\ N_o(D_a + D_b)(r_a + r_b)}{1000} \qquad (35)$$

where D_a+D_b are the diffusion coefficients (cm^2/s) for reacting molecules a and b, r_a and r_b are their molecular radii (cm), and N_0 is Avogadro's number. In terms of naphthalene sorption to HA, Values of D_a and D_b can be estimated from [21]

$$D = \frac{13.26x10^{-5}}{\mu^{1.14} V_m^{0.589}} \qquad (36)$$

where μ is the viscosity of water (0.894 x 10^{-2} g cm^{-1} s^{-1}) and V_m is the molar volume of naphthalene (~130 cm^3/mol) or HA (41667 cm^3/mol). The resulting diffusion coefficients for naphthalene and HA molecules are D_{Nap}=8.6 x 10^{-6} cm^2/s and D_{HA}=2.9 x 10^{-7} cm^2/s, respectively. The value for naphthalene is typical of HOCs, which have diffusion coefficients on the order of 10^{-5} cm^2/s. This means that the contribution of D_{HA} to Z can be generally ignored in considering sorption to HA. The value of the radii for a HA molecule (r_{HA}) is estimated at 1.5 x 10^{-6} cm [5], while the value of the radii for a naphthalene molecule (r_{Nap}) is estimated at V_{Nap} at 3.6 x 10^{-8} cm, assuming naphthalene occurs as a sphere. Since r_{HA}>>r_{Nap}, the collisional frequency between HA and naphthalene at unit concentration becomes

$$Z = \frac{4\pi\ N_o(D_{Nap})r_{HA}}{1000} \qquad \text{(L/mol s}^{-1}\text{)} \qquad (37)$$

Adjusting the units of Z to be (min^{-1} L/kg DOC) yields

$$Z = \frac{4\pi\ N_o(D_{Nap})r_{HA}}{M_{HA}fc} \tag{38}$$

where M_{HA} is molecular weight of HA (~50,000 g/mol). Assuming each collision between naphthalene and HA in solution results in sorption therefore yields $k_s=10^7$ (min^{-1} L/kg of DOC) for naphthalene.

A maximum value for k_d can be constructed similarly using

$$Z_d = \frac{D_{NAP}}{\pi r^2_{HA}} \tag{39}$$

if it is recognized that HOCs sorbed to HA diffuse freely within the aqueous HA matrix. Assuming that HOC diffusion coefficients in water and in the aqueous HA matrix are the same, and if diffusion out of HA defines desorption, then under these conditions, $k_d = Z_d = 2.7 \times 10^6\ min^{-1}$ for naphthalene desorption. Given the maximum values of k_s and k_d, and the simulation illustrated in Figure 9, then even with diffusion-controlled exchange, naphthalene volatilization from HA solution having a DOC concentration of 1710 mg/L would be expected to be significantly retarded relative to solution with HA (provided K_{DOC}=880).

The effect of changing K_{DOC} on naphthalene volatilization is illustrated in Figure 10. As in Figure 9, the observed behavior is indicated by data points. Setting $k_s=1.7 \times 10^2\ min^{-1}\ (kg\ DOC/L)^{-1}$ and $k_d=k_d/K_{DOC}$ yields the solid line in Figure 10 when K_{DOC} equals 880. Keeping the value of k_s fixed, increased K_{DOC} values result in increased volatilization rate retardation, while decreased K_{DOC} values result in decreased volatilization rate retardation. These results also are in agreement with the current understanding that HA-sorbed molecules can not exchange directly with the gas phase. As K_{DOC} is decreased, and with it the initial fb, the result is that the

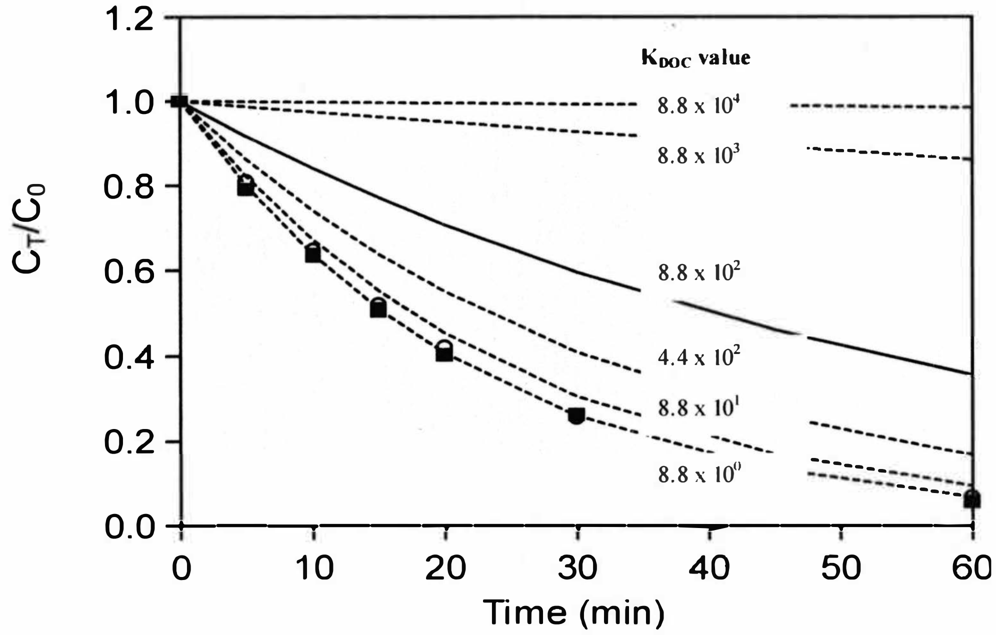

Figure 10. Expected Curves for Naphthalene Volatilization From HA Solution Given Fixed k_s (k_s=1.7 x 10^2).

distinction between HA and aqueous solutions vanishes as less and less naphthalene is affected by the presence of HA. Volatilization rate retardation in HA solution consequently appears to be defined primarily by the value of fb in the initial HA solution, provided that HA-sorbed HOCs cannot exchange directly with the atmosphere. If this is true, then the experimental results obtained for naphthalene and most of the other compounds indicate that much less of those compounds is sorbed to

HA in the HA solutions than is predicted from the K_{ow}-based K_{DOC} values.

Effect of DOC on K_{DOC} Values

Many of the sparging experiments were conducted at HA concentrations much greater than typically found in the environment. Values in natural water range from 1-100 mg/L DOC, with most values (>90%) falling below 5 mg/L DOC. The high DOC concentrations used in the current work were nevertheless used because the K_{ow}-based K_{DOC} values indicated that significant sorption to HA was possible for some compounds only at the higher HA concentrations. Preliminary analysis of K_{DOC} values obtained at multiple DOC concentrations suggests that volatilization rates from HA

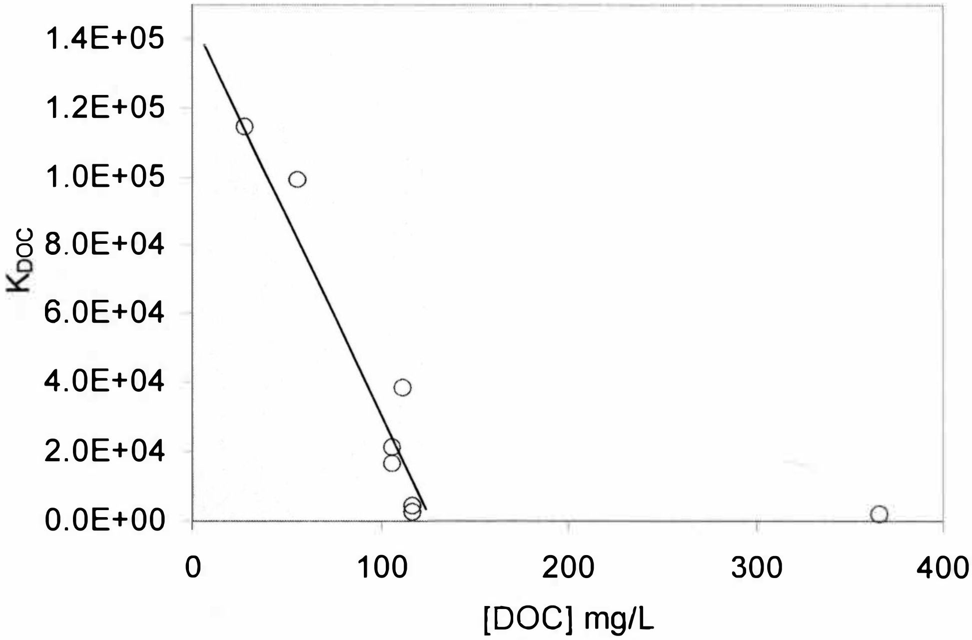

Figure 11. DOC Concentration Effect on HCB K_{DOC} Values.

solution are affected by DOC concentration. Apparent K_{DOC} values for HCB in HA solution are summarized in Figure 11 plotted against DOC. Linear regression of the values against DOC (excluding the value after 117 mg/L) yielded $K_{DOC}=-1250.8[DOC]+157121$, with 95% of the variance (r=0.967, n=7) being explained by the regression equation. The resulting K_{DOC} value at 1 mg/L DOC corresponds to 1.6×10^5 , versus 1.3×10^5 predicted from the K_{ow}-base K_{DOC} value [21].

Variation in K_{DOC} with DOC concentration is unexpected since K_{DOC} is held to be independent of DOC concentration. Nevertheless, other authors (c.f. [29]) also have reported K_{DOC} changes over the range of 0-100 mg/L DOC.

K_{DOC} From Apparent Henry's Law

Apparent Henry's Law

To assess the effect of DOC on apparent K_{DOC} values (K_{DOC}') measuremed in the current work, K_{DOC} values were determined from sparging data using the idea of apparent Henry's Law. This method was used, rather than curve-fitting to Equations 26-32, because the multi-compartment model relies on estimates of k_s and k_d to determine K_{DOC}. The alternative method for determining K_{DOC} is based on the definition for Henry's law constant (H) such that

$$H=\frac{C_g}{C_d} \qquad (40)$$

where C_g and C_d are the equilibrium concentrations of compound in the gas phase and dissolved phase, respectively. In the case of HA solution, an apparent H (H') can be defined by

$$H' = \frac{C_g}{C_d + C_s} \tag{41}$$

where C_s is the equilibrium concentration of solute in the HA-sorbed phase. Using the definition of K_{DOC} in Equation 3, and combination with Equation 40 and 41 yields

$$K_{DOC} = \frac{(\frac{H}{H'} - 1)}{[DOC]} \tag{42}$$

According Mackay et al. [45], H can be related to the rate constant for volatilization in absence of DOC (k_v), and H' can be related to the rate constant of apparent volatilization in presence of DOC (k_v'), via

$$kv = \frac{H\,Q}{V} \tag{43}$$

and

$$kv' = \frac{H'Q}{V} \tag{44}$$

where V (L) is a volume of solution, and Q (L/min) is the volumetric gas flow during sparging. The rate of change in total solution concentration (C_T) with time during sparging is therefore

$$\frac{dC_T}{dt} = k_v C_T \tag{45}$$

in solution without HA and

$$\frac{dC_T}{dt} = k_v' C_T \tag{46}$$

in solution with HA.

Figure 12 illustrates the results of curve-fitting Equation 46 to data for HCB in HA solution containing 112 mg/L DOC. The dashed line through the data points represent the first-order fit of Equation 46 to the full data set while the solid line represents the first-order fitting of Equation 46 to data for $t<30$ min. As Figure 12 shows, curve-fitting to the full data set results in a line that deviates from the data after $t=15$ min. Using the truncated data set, on the other hand, leads to deviation after 30 min. Curve-fitting of Equation 46 to the full time series yields $K_{DOC}=1890$, while the truncated data series yields $K_{DOC}=970$. The larger K_{DOC} value from the full data set is expected because of the influence of the later data in defining the curvature of the fit (i.e., k_v').

Deviation from first-order kinetics as C_T/C_0 approached zero was a common result for all compounds in all sparging experiments. This same deviation has been reported previously for sparging of HOCs from HA solution and has been attributed to a variety of causes (c.f., [29]). In the current work, K_{DOC} values determined from application of Equations 42-46 to sparging data were based on curve-fits to truncated data sets comprised of C_T/C_0 values ≤0.6.

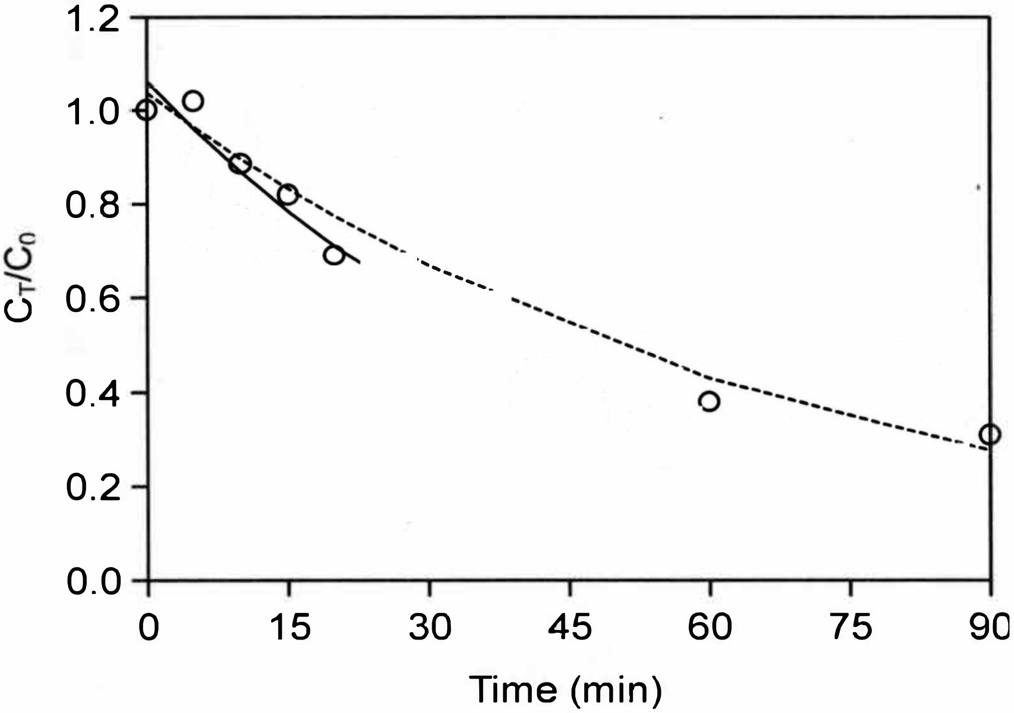

Figure 12. Comparison of Curve-Fitting Approaches to HCB Time Series Data.

Chlorinated Benzenes

Application of the Henry's law-based methods for estimating K_{DOC} values for chlorobenzenes are illustrated in Figures 13-17. In these Figures, K_{DOC} values determined from truncated time series are presented as apparent K_{DOC} values (K_{DOC}'). Error bars in the Figures represent standard errors for K_{DOC}' values. Significant differences in K_{DOC}' values occurred for the chlorinated benzenes as DOC concentration was changed. In the case of HCB, for example, K_{DOC}' is $6.8 \pm 0.6 \times 10^4$

at a DOC concentration of 28 mg/L, while K_{DOC}' is $3.5 \pm 0.3 \times 10^3$ at a DOC concentration of 120 mg/L. This K_{DOC}' difference is more than an order of magnitude. As a consequence, this difference can not be explained by experimental variance, which was 14%. Therefore, the decrease observed in K_{DOC}' with changing DOC concentration is statistically significant. The change in K_{DOC}' with DOC concentration for the five chlorinated benzenes is most pronounced at DOC concentrations ≤200 mg/L. At higher DOC concentration values, K_{DOC}' values commonly approached zero. This limit is a consequence of the disappearance of volatilization rate retardation at high DOC concentration. This is illustrated by example rate plots for TCB in Figure 18. At a DOC concentration of 370 mg/L, TCB volatilization apparently is accelerated in HA solution relative to solution without HA, yielding $K_{DOC}'=-6.2 \times 10^2$. The

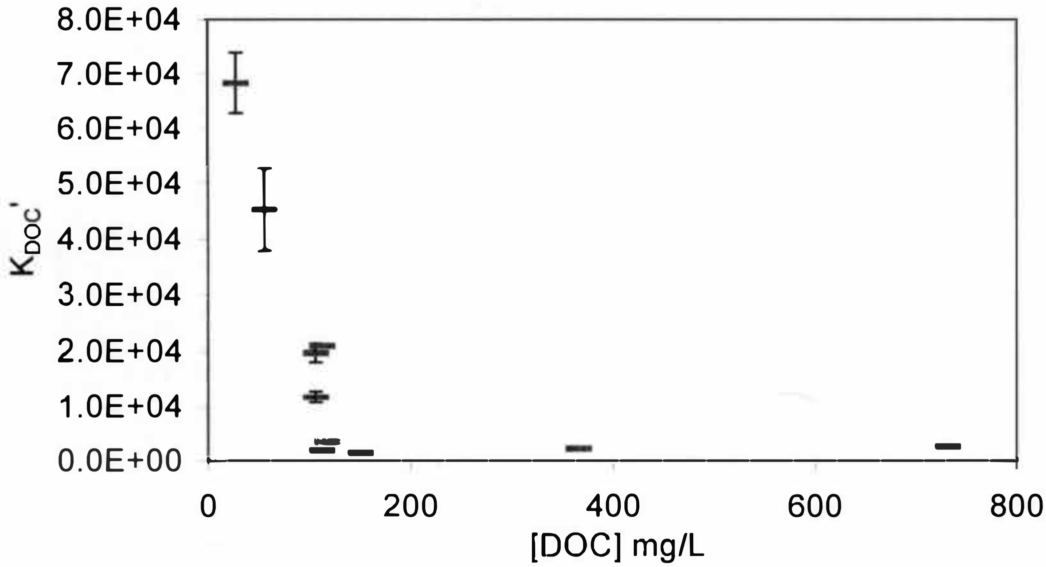

Figure 13. Change in HCB K_{DOC}' With DOC Concentration.

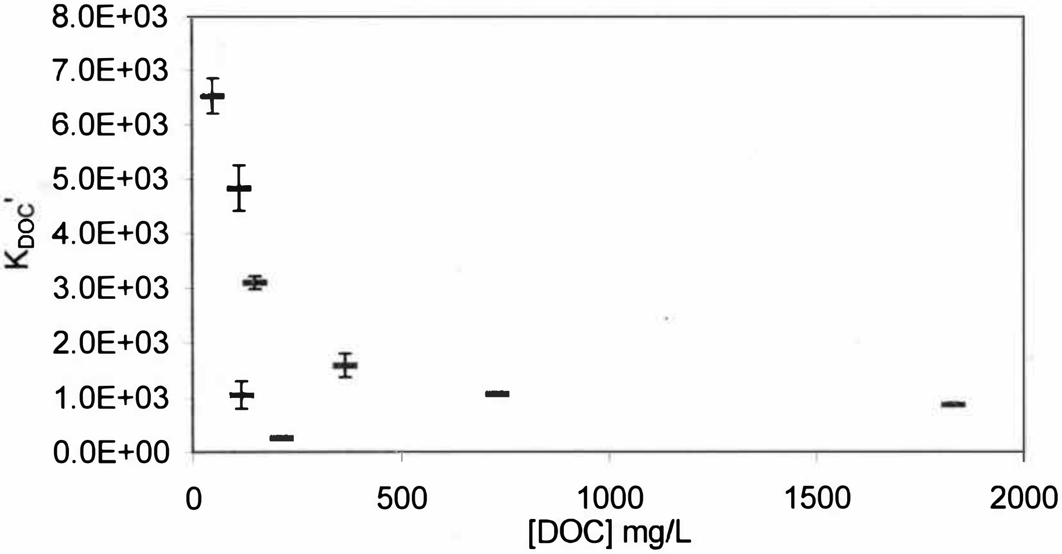

Figure 14. Change in QCB K_{DOC}' With DOC Concentration.

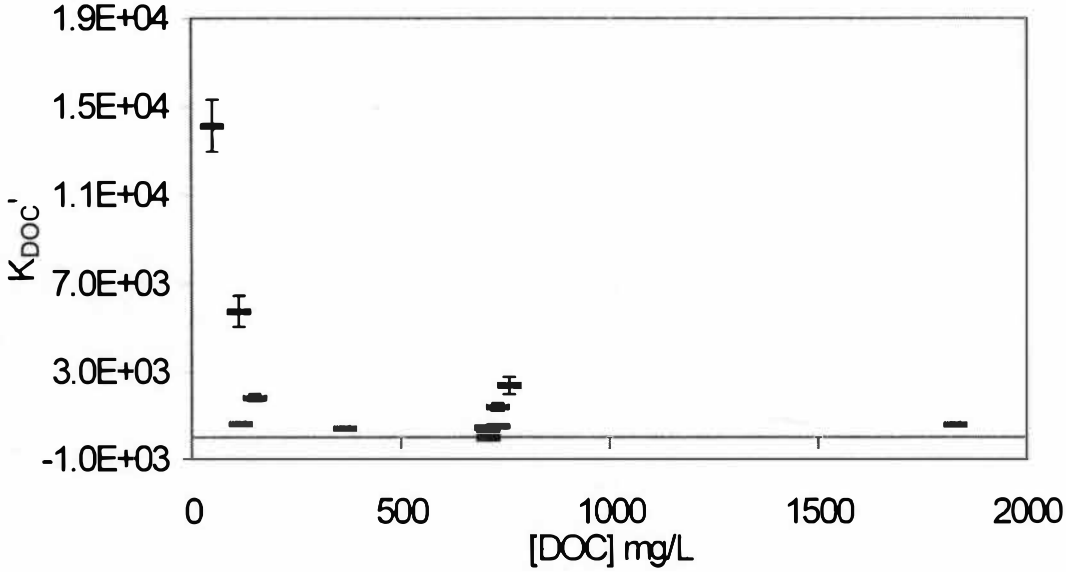

Figure 15. Change in TeCB K_{DOC}' With DOC Concentration.

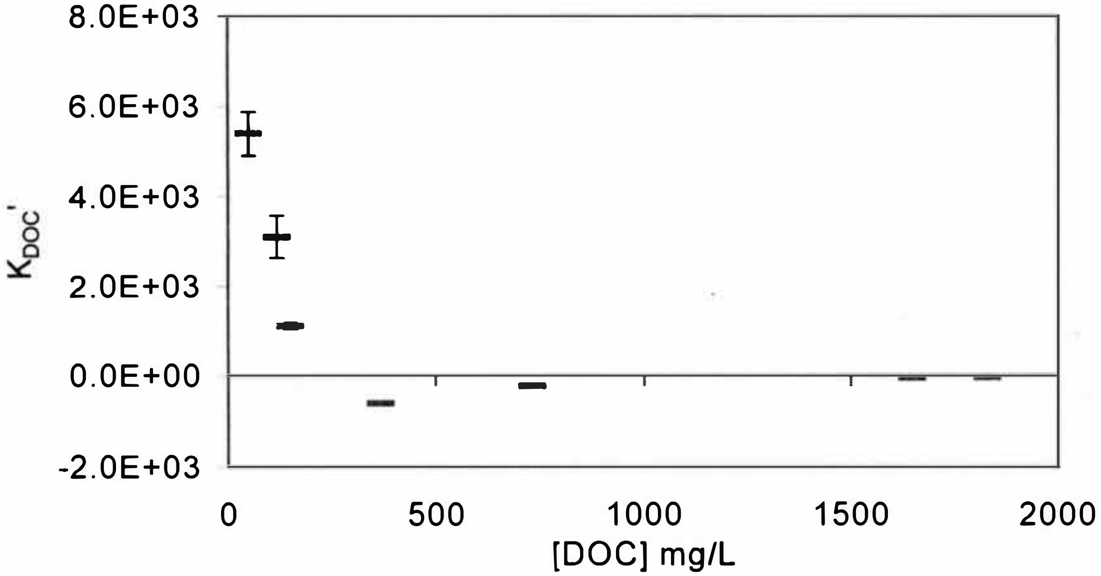

Figure 16. Change in TCB K_{DOC}' With DOC Concentration.

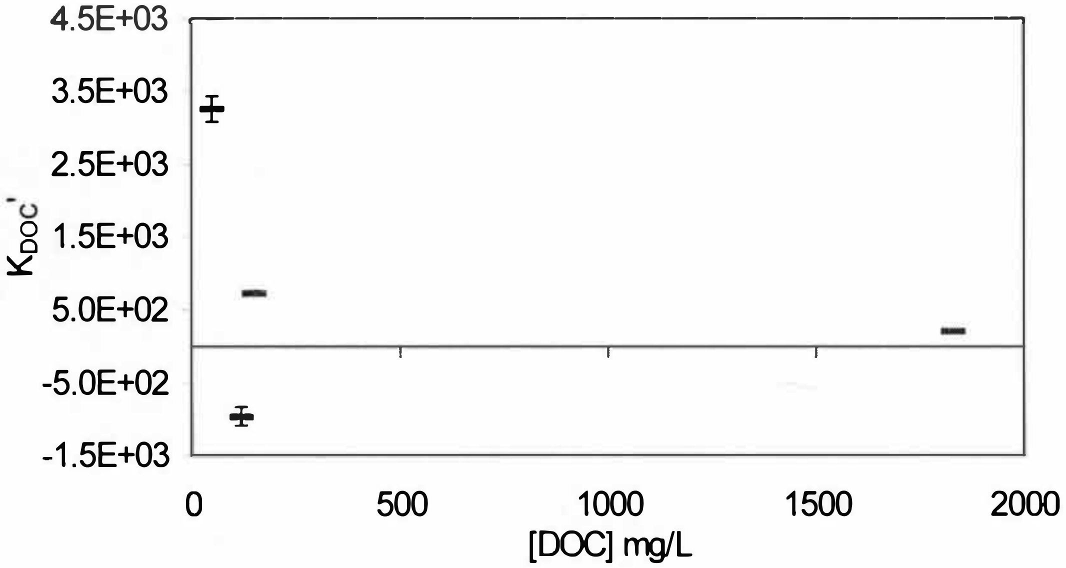

Figure 17. Change in DCB K_{DOC}' With DOC Concentration.

general observation that volatilization rate retardation decreases and then disappears with increasing DOC concentration suggests that HOC sorption to HA also decreases with increasing DOC concentration, since gas exchange is presumed to be possible only for dissolved phase solutes.

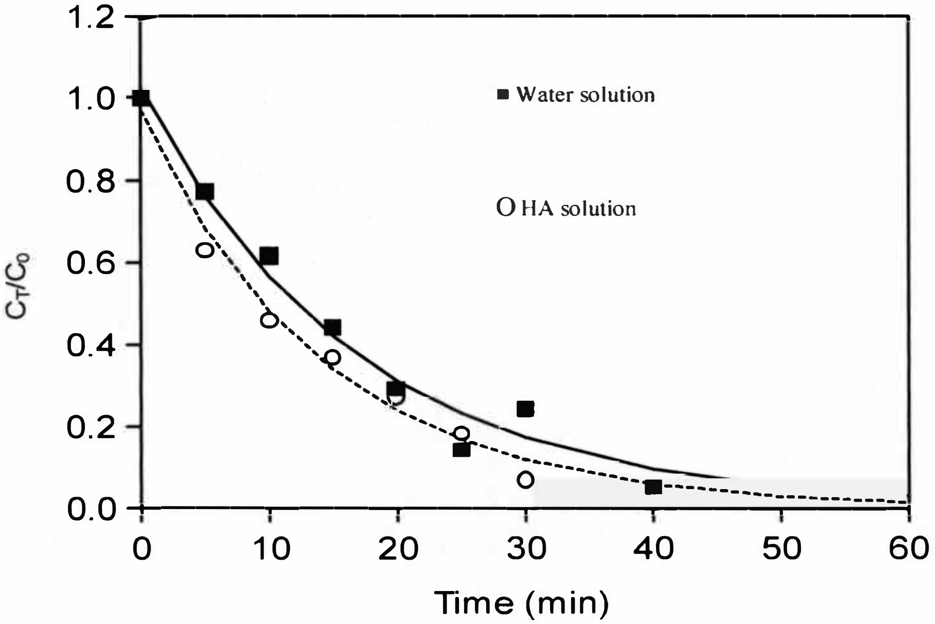

Figure 18. Rate Plot for Change in TCB Concentration (C_T) Relative to Initial Value (C_0) in HA and Water Solutions.

Comparison With Other Work

Natural waters typically do not exceed DOC concentrations of 100 mg/L. As a consequence, most measurements of K_{DOC} have been performed at DOC concentrations<100 mg/L. For example, K_{DOC} values determined using fluorescence techniques typically use DOC concentrations<30 mg/L (c.f., [47]). The basis for the fluorescence techniques is quenching of HOC fluorescence on binding to HA. K_{DOC} is measured in these techniques from linear Stern-Volmer plots, which translate into a constant K_{DOC} with DOC concentration. However, because HAs fluoresce and also absorb light, use of this technique is restricted to low DOC concentration. At these concentrations, and using this technique, K_{DOC} values have proven to be constant with DOC concentrations. Gauther et al. [43] for example, measured K_{DOC} values for PAHs over DOC concentration of 4-24 mg/L. The linear regressions in Stern-Volmer plots all showed r=0.999, suggesting that K_{DOC} is constant in this DOC concentration range. Results obtained with other techniques have been similar. For example, Evans [47] reported no change in K_{DOC} with DOC concentration=1-6 mg/L for PCB 52 and PCB 153 using a reversed-phase HPLC separation technique. Similarly, Gshwend and Wu [48] used a batch equilibration technique to measure K_{DOC} values for PCBs. In these experiments, the DOC was released from soils on mixing with water. Soil concentrations in the experiments were 10 to 10000 mg/L, corresponding to DOC concentrations of 0.25 to 125 mg/L. Considering the dissolved and soil-based ("particulate") organic carbons separately, constant K_{DOC} values were observed over the full concentration range. Reports that K_{DOC} varies with DOC concentration nevertheless exist. For example, McCarthy and Jimenez [49] utilized an equilibrium dialysis technique to investigate the effect of DOC concentration on K_{DOC} values for a series of PAHs (i.e., benzo[a]pyrene, benzanthracene, anthracene and naphthalene). K_{DOC} values for benzo[a]pyrene, anthracene and benzanthracene were found to decreases ~30-50 %, when the DOC concentration was increased from 1 mg/L to <80 mg/L. For naphthalene, a change in K_{DOC} value of ~20 % was observed over the range at 1-300 mg/L DOC.

K_{DOC}' vs DOC Concentration Linear Regression Analysis

Linear regressions of K_{DOC}' values vs DOC concentrations ≤250 mg/L appear in Figure 19-23. Error bars in plots are standard errors for K_{DOC}' values, while lines through data points are best-fit regressions of K_{DOC}' vs DOC concentration. In all cases, regression slopes were negative and the ratio of slope to intercept was ~0.8, meaning that a change in DOC concentration 10 mg/L corresponds to a change in K_{DOC}' of ~8%.

K_{DOC}' values determined using gas sparging have previously been reported to decrease with increasing DOC concentration. Hassett and Milicic [29] for example, found that the K_{DOC} value for 2,2',5,5'-tetrachlorobiphenyl (PCB 52) varied with DOC concentration over the range 5-50 mg/L. Based on the assumption that apparent K_{DOC} values at the lowest DOC concentrations were elevated due to HOC sorption to vessel walls during sparging, Hassett and Milicic plotted K_{DOC} vs 1/DOC concentration and used the intercept at high DOC concentration to define the "actual" K_{DOC} value. However, the resulting "actual" K_{DOC} was 7.1×10^4, which is 14 % of the K_{ow}-based K_{DOC} value (5.2×10^5, ref 21). In contrast, the K_{DOC} value obtained at a DOC concentration of 5 mg/L was 2.5×10^5, in good agreement with the K_{ow}-based K_{DOC} value. Similar results have been reported by Pardue et al. [50] for HCB at DOC concentrations of 10-115 mg/L. Also based on assumption that high K_{DOC} values at low DOC were due to HOC sorption to glass, Pardue et al. [50] concluded that the

K_{DOC} value at high DOC concentration was the "actual" K_{DOC} value. The resulting value, 2.4 x 10^4, is 18 % of the K_{ow}-based K_{DOC} value (1.3 x 10^5, ref 21). In contrast, the K_{DOC} value obtained at DOC concentration of 10 mg/L was 1.0 x 10^5, in good agreement with the K_{ow}-based K_{DOC} value.

K_{DOC} values based on regression equations at 1 mg/L DOC for the chlorinated benzenes (Figures 19-23) are compared with the K_{ow}-based K_{DOC} values in Table 3 and Figure 24. In general, there is good agreement between values, suggesting that K_{DOC} values determined using gas sparging are most accurate at low DOC concentration, rather than high DOC concentration, as suggested by Hassett and Milicic [29] and Pardue et al. [50].

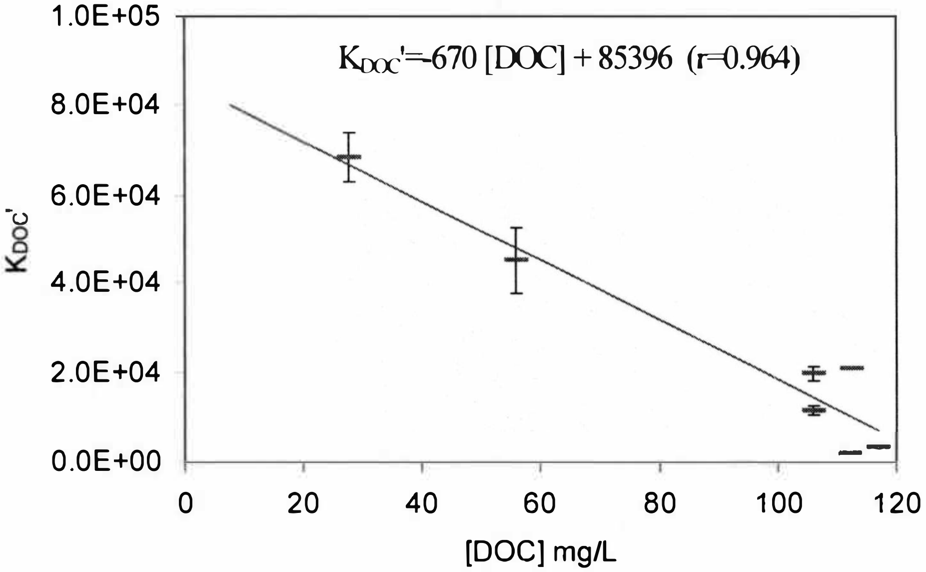

Figure 19. Linear Regression of HCB K_{DOC}' vs DOC Concentration.

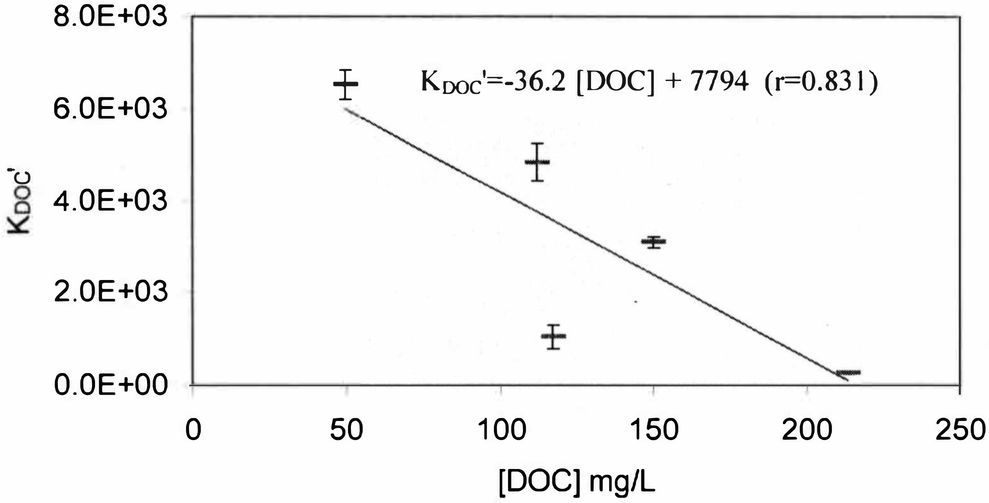

Figure 20. Linear Regression of QCB K_{DOC}' vs DOC Concentration.

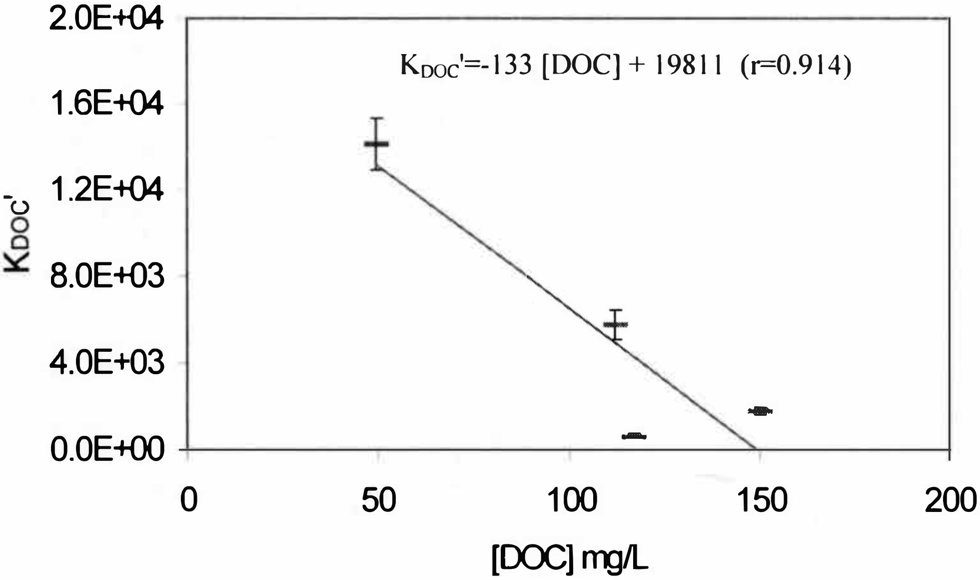

Figure 21. Linear Regression of TeCB K_{DOC}' vs DOC Concentration.

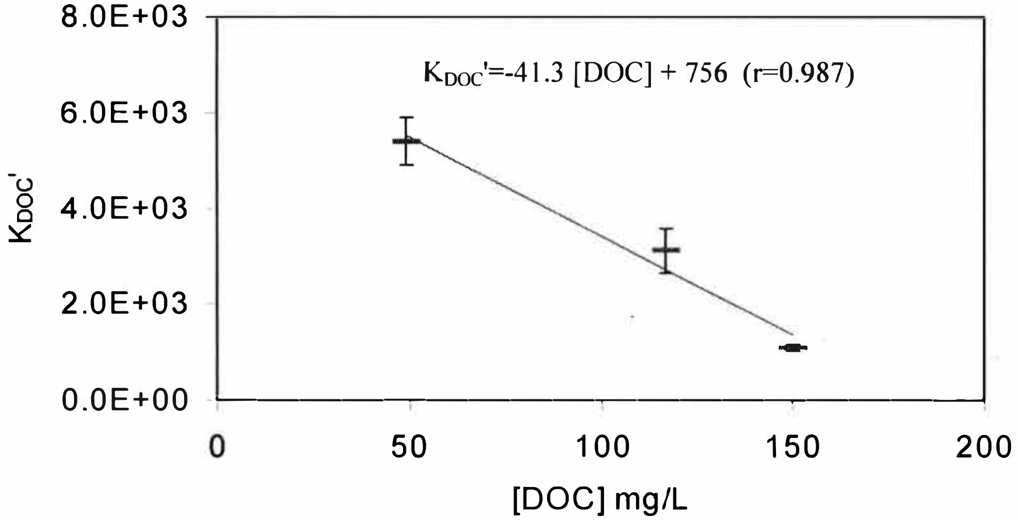

Figure 22. Linear Regression of TCB K_{DOC}' vs DOC Concentration.

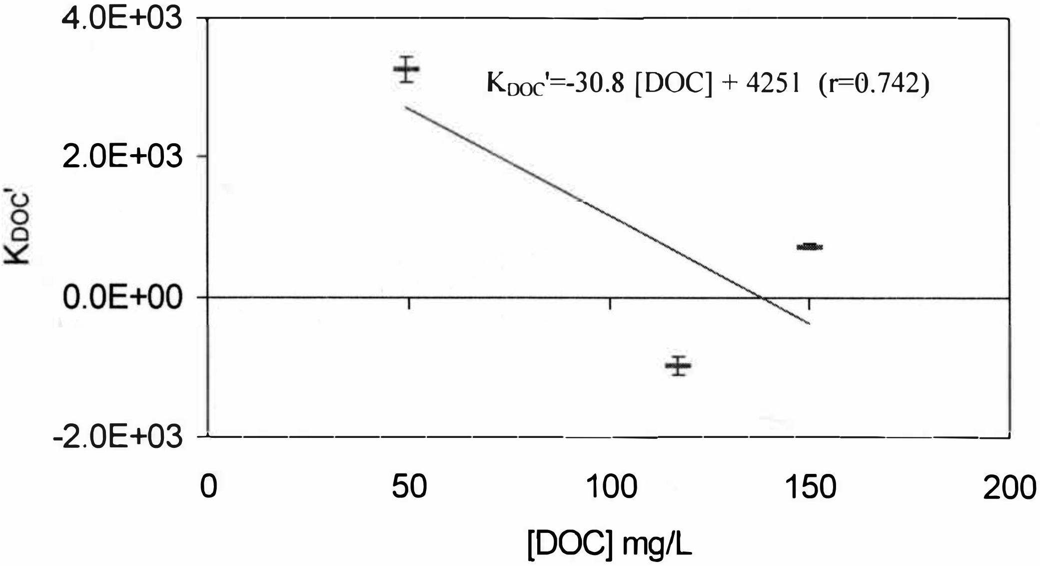

Figure 23. Linear Regression of DCB K_{DOC}' vs DOC Concentration.

Table 3

Chlorinated Benzenes Regression-Based K_{DOC}' and K_{ow}-Based K_{DOC} Values

Compound Name	Regression-Based K_{DOC}'	K_{ow}-Based K_{DOC}*
DCB	4.3×10^3	1.0×10^3
TCB	7.6×10^3	5.2×10^3
TeCB	2.0×10^4	1.3×10^4
QCB	7.8×10^3	4.1×10^4
HCB	8.5×10^4	1.3×10^5

* K_{ow} values from ref [21]

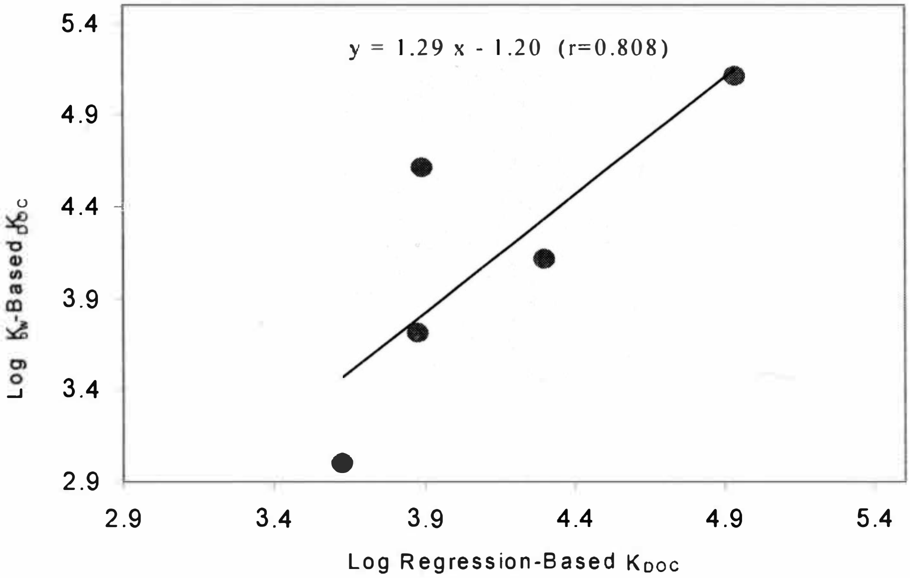

Figure 24. Correlation Between Chlorinated Benzene K_{ow}-Base K_{DOC} and Regression-Based K_{DOC}' Values Estimated by Linear Regression.

Gas Sparging and K_{DOC}

Mass Transfer Between Solution and Gas Phases

The use of gas sparging to measure K_{DOC} values is based on a series of assumptions. The first of these is illustrated conceptually in Figures 25-27. Figure 25 illustrates solute mass transfer during gas sparging of aqueous solution containing no HA. In this figure, dissolved phase solute molecules are indicated by S_d, while gas phase solute molecules are indicated by S_g.

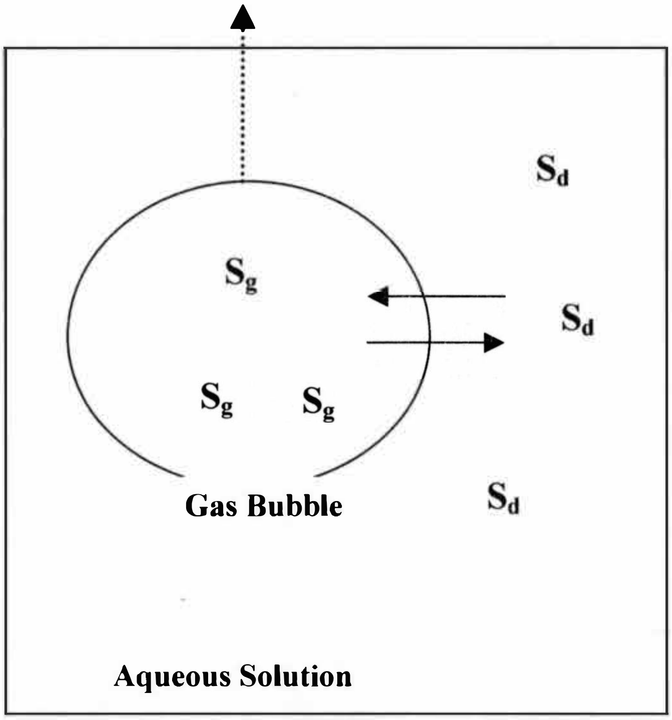

Figure 25. Mass Transfer of Solute Between Aqueous Solution and Gas Phase.

For HOCs, the rate of mass transfer from liquid to gas phase is liquid phase controlled (c.f., [45, 46]). Assuming first-order mass transfer during vertical gas flow along the length of a bottle, the change in concentration of HOC in gas bubbles (C_g) is described by [51]

$$\frac{dC_g}{dz} = \frac{K_L a_b A}{Q}\left(C_d - C_i\right) = \frac{K_L a_b A}{Q}\left(C_d - \frac{C_g}{H}\right) \tag{47}$$

where C_d is the bulk solution concentration of HOC, C_i is the concentration of HOC in water at the gas-water interface, K_L is the diffusional liquid mass transfer coefficient (m/s), a_b is the specific bubble surface area per unit solution volume (m^2/m^3), A is the cross section area of the bottle (m^2), Q is the volumetric gas flow (m^3/s), z is the depth of bubble introduction (m), and H is the dimensionless Henry's constant. Since gas entering the bottom of the bottle is free of HOC, integration of C_g with respect to z yields

$$C_g = H\, C_d\left(1 - e^{-\alpha}\right) \tag{48}$$

where α is

$$\alpha = \frac{K_L a_b A z}{Q\, H} \tag{49}$$

This solution assumes that during its life-time, a bubble is in contact with water containing a constant concentration of HOC. The mass balance over the time course of an experiment yields

$$-V\frac{dC_d}{dt} = H\,C_d(1-e^{-\alpha})Q \tag{50}$$

where V is the volume of solution (m^3). Integration of Equation 50 yields

$$\ln\left(\frac{C_d}{C_0}\right) = -\frac{H\,Q\,t}{V}(1-e^{-\alpha}) \tag{51}$$

where C_0 is the initial concentration of HOC in solution.

Under experimental conditions leading to equilibrium between gas bubbles and solution (e.g. large z, large A, small Q), the exponential function in Equation 51 becomes negligible so that

$$\ln\left(\frac{C_d}{C_0}\right) = -\frac{H\,Q\,t}{V} \tag{52}$$

This yields the same equation derived by Mackay et al. (Equations 43 and 45, ref 45), so that a plot of $\ln(C_d/C_0)$ vs time is linear with a slope of -(HQ/V), where HQ/V is the rate constant for volatilization, k_v.

Figure 26 illustrates solute mass transfer during gas sparging of HA solution. In this Figure HA-associated molecules are represented as S_s. As illustrated in this Figure, there is no exchange between HA and gas phase. This assumption was first introduced by Mackay and Shiu [45] based on their observation that the rate of naphthalene volatilization in HA solution was retarded relative to solution without HA. Hassett and Milicic's [24] description for mass transfer from HA solution to the gas phase during sparging experiments is based on this assumption (Equation 26-29).

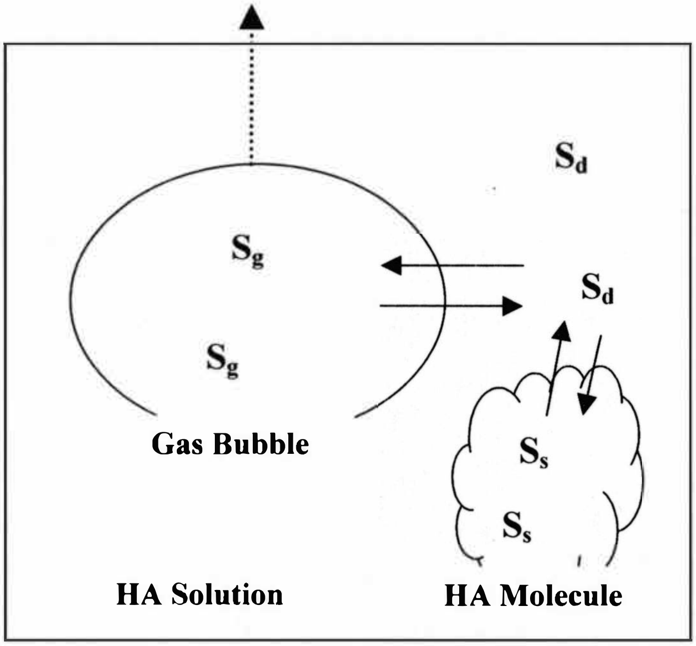

Figure 26. Mass Transfer of Solute Between HA Solution and Gas Phase.

Under conditions where there is equilibrium between dissolved and HA phases, dissolved and gas phases, but not HA and gas phases, Hassett and Milicic [29] proposed that mass transfer from HA solution to the gas phase could be represented by

$$\ln\frac{C_T}{C_0} = -\frac{k_v t}{1 + K_{DOC}[DOC]} \tag{53}$$

where C_T is the total concentration of HOC in HA solution at time t, and C_0 is the total concentration of HOC in HA solution at t=0. This equation is the same as that leading to the use of H' to calculate K_{DOC} (Equations 44-46). In either case, volatilization rate retardation in HA solution is represented as being a constant function of DOC concentration, with K_{DOC} values defining that constant function. The repeated observation that K_{DOC} values from gas sparging are not a constant function of DOC concentration suggests that the assumption behind these experiments may not be correct.

Mass Transfer Between HA and Gas Phases

HAs have been known for some time to be surface active compounds capable of altering aqueous solution surface tension by accumulating at air-water interfaces [52]. Wan and Tokunaga [53] used a bubble-fractionating column to measure the partition coefficient describing the surface excess of HA at the air-water interface (K). Using salts to measure the column eddy dispersion coefficient, and confirming partition coefficients with independent measures based on surface tension, K for soil humic acid 1S102H (International Humic Substance Society) was found to be 27 ± 6 μm, meaning that the mass of HA per unit air-water interfacial area was the same as the mass found per unit area in a bulk solution thickness of 27 μm.

Concentration of HA molecules at the air-water interface brings sorbed HOC molecules to that interface as represented in Figure 27. If these HOC molecules undergo HA-gas exchange, then K_{DOC} values measured by gas sparging would be expected underestimate actual K_{DOC} values by a factor equal to the exchanging population. This population can be described as being a function of the fraction of the total HA molecules at the air-water interface and the number of HOC molecules per

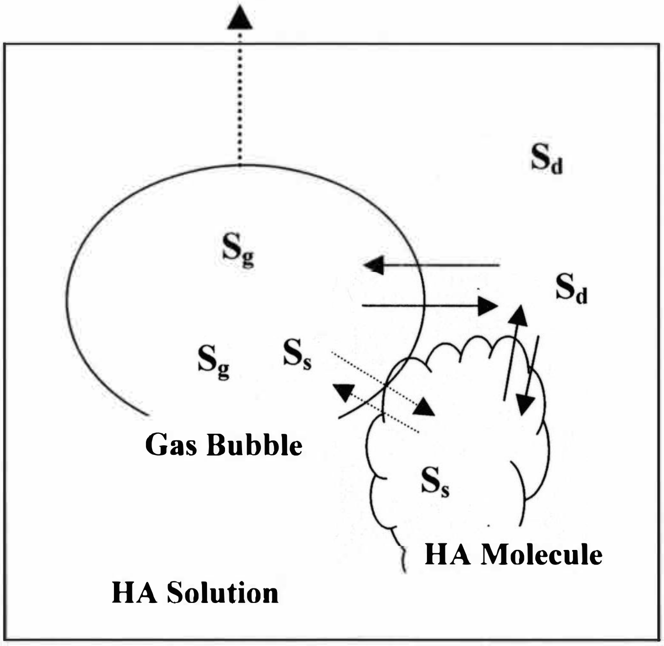

Figure 27. Mass Transfer of Solute Between HA Solution and Gas Phase Based on HA Accumulation at the Air-Water Interface.

HA molecule. As a first approximation, for a given system and constant conditions, the fraction of the total HA molecules at the air-water interface is expected to be directly proportional to the bulk solution HA concentration (Wan and Tokunaga [53]). Similarly, the molecular concentration of sorbed HOC capable of HA-gas exchange is expected to be proportional to the sum of the probabilities for HOC occupancy in HA molecules (Pr_n). The resulting dependence of apparent K_{DOC} values on DOC concentration is

$$K_{DOC}' = \frac{C_s - X[DOC]\sum_{n=1}^{n=\infty} Pr_n}{C_d[DOC]} \tag{54}$$

where X is the overall proportionality constant. Figure 28 shows the results of fitting Equation 54 to HCB K_{DOC}' data for DOC concentrations<400 mg/L. The fit is in good agreement with observation, suggesting that direct HA-air exchange could produce the decrease in K_{DOC}' with DOC concentration that is observed.

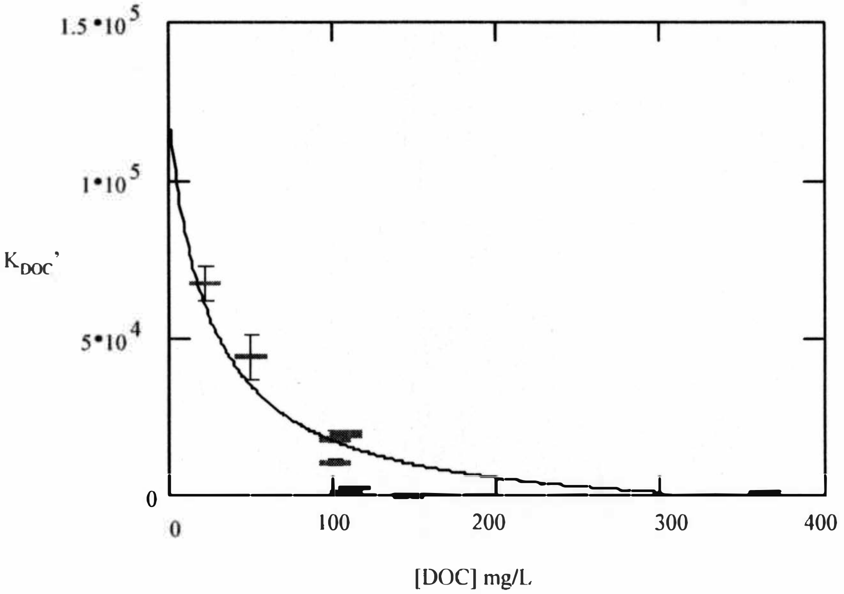

Figure 28. Predicted and Observed Effect of DOC on HCB K_{DOC}' Values.

Equation 54 applies to fixed systems with constant conditions such as bubble size and gas flow. Changing system conditions would be expected to change the K_{DOC}' values determined by gas sparging, if there is HA-air exchange of HOC molecules sorbed at the air-water interface. Figure 29, for example, shows how a 34 % decrease in bubble size, and therefore a 50 % increase in volume per interfacial area, affects the dependence of K_{DOC}' on DOC concentration. Wan and Tokunaga [53] observed changes in bubble size of this magnitude in their bubble-fractionating

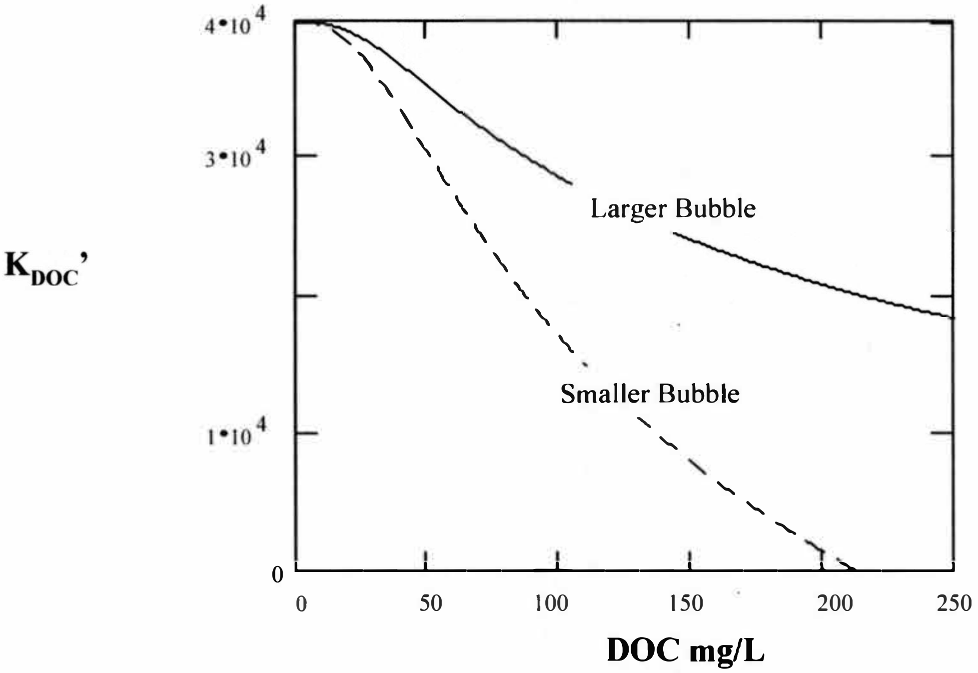

Figure 29. Predicted Effect of Gas Bubble Size on K_{DOC}' Values.

column by changing the salt concentration in HA solution. NaCl concentrations of 1.0 x 10^{-3} and 1.0 x 10^{-1} M yielde bubble diameters of 638 μm and 539 μm, respectively. The increased curvature in Figure 29 is a result of increased X in Equation 54. Decreasing bubble size is consequently predicted to result in lower K_{DOC}' values measured using gas sparging. In agreement with this prediction, K_{DOC}' values for QCB were smaller when a diffuser (60 μm pore size) was added to the gas inlet (1/8") in sparging bottles (Figure 30). The gas diffuser has the effect of reducing bubble size for a given gas flow. The agreement between prediction and observation again suggests that direct HA-air exchange may be occurring during gas sparging of HA solutions.

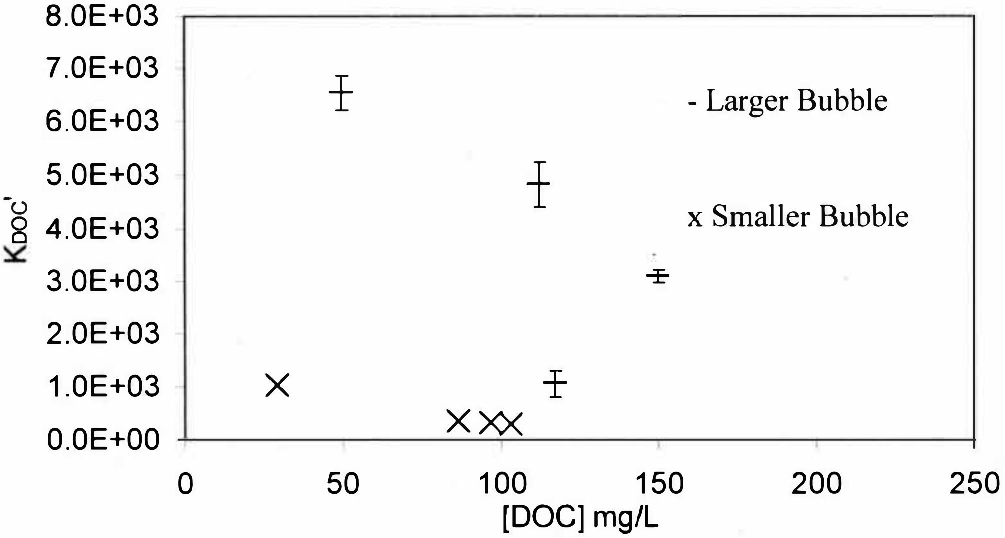

Figure 30. Observed Effect of Gas Bubble Size on QCB K_{DOC}' Values.

CHAPTER IV

CONCLUSIONS

Gas sparging has been accepted as a viable method for distinguishing between humic acid-associated (HA-associated) and non-associated hydrophobic organic compounds (HOCs) in aqueous solution, and therefore is one of the accepted techniques used to measure HOC-HA partition coefficients (K_{DOC}). However, K_{DOC} values measured using gas sparging commonly vary with dissolved organic carbon (DOC) concentration (c.f., [54, 55]), as in the current work, even though current theory offers no explanation for the variation.

In other reports of K_{DOC} decreases with DOC concentration, researchers commonly have supposed that K_{DOC} values measured at higher DOC concentrations are more accurate than those measured at lower DOC concentrations (c.f., [29, 50]). "Actual" K_{DOC} values in that body of work consequently are commonly obtained from the intercept of plots of K_{DOC} vs 1/DOC concentration. The resulting "actual" K_{DOC} values invariably have been significantly lower than K_{DOC} values expected based on the observation that $K_{DOC} \approx 0.41\ K_{ow}$ [35]. At the same time, K_{DOC} values obtained at low DOC concentration have proven to be better matched with K_{ow}-based values.

One major difference between previous work and the current work is the range of DOC concentrations used in sparging experiments. In the current work, DOC concentrations as high as ~2000 mg/L DOC were used in experiments. In previous work, concentrations rarely exceeded 100 mg/L DOC [29, 31, 54, 55, 56]. At the very high DOC concentrations used in the current work, the volatilization rate retardation expected based on sorption to DOC was not apparent. Instead, K_{DOC} values approached zero as DOC concentration was increased. In previous work, because only low DOC concentration were used, this limit was not observed [29, 50]. As a result, researchers assumed that once the HA-bound fraction (fb) of HOC was >0.9, apparent K_{DOC} values would no longer change with DOC concentration. The limit of DOC concentrations defined in that previous work consequently was that where fb>0.9 was expected.

Linear regression of K_{DOC}' vs DOC concentration yields K_{DOC} values at 1 mg/L DOC that are in good agreement with the expected K_{ow}-based K_{DOC} values, suggesting that values at higher DOC concentration are deviating from the "actual" K_{DOC}. Additionally, the regression-based K_{DOC} values are slightly higher than K_{ow}-based K_{DOC} values. Experimentally measured K_{DOC} values higher than K_{ow}-based K_{DOC} values (K_{oc} values) have previously been reported by Wijayaratne and Means [57], for PAHs. Assuming no HOC exchange between HA and gas phases, then changes in K_{DOC} values with DOC concentrations measured using gas sparging are possible only if sorption actually is changing with DOC. Such a "change" is not observed using alternative methods for measuring K_{DOC}. If sorption to DOC does not change with DOC concentration, then changes in K_{DOC}' with DOC concentration, during sparging experiments must have another cause. An alternative cause is that HOCs undergo HA-gas exchange, and that the population of exchanging HOC molecules increases with DOC concentration.

Comparison of observed and expected variation in K_{DOC} with DOC concentration, assuming HA-gas exchange, yields results that are in good agreement. Additionally, qualitative agreement is found for the predicted and observed variation in K_{DOC} values with changing gas bubble size.

Direct solute mass transfer between gas and HA phases makes gas sparging methodology not viable for measuring K_{DOC} or k_s and k_d, This is because the additional solute mass transfer pathway introduces another parameter into Equations 26-32. With this additional parameter, Equations 26-32 cannot be solved without the ability to independently describe the additional mass transfer pathway.

HA-gas exchange has tremendous significance in terms of the fate of HOCs in natural waters, especially in places where bubbles are generated, such as waterfalls. Previously, HA-gas exchange of HOCs was not included in predictions of the fate of HOCs from aqueous phase to the atmosphere. This HA-gas exchange will yield higher inputs of HOCs into the atmosphere from water bodies than previously expected.

REFERENCES

1. Boogs, S. J.; Levermore, D. G.; Seitz, M. G. Humic macromolecules in natural waters, *J. Macromol. Sci. Rev.* 1985, **25**(4), 599.

2. Cornelium, S. What is humic acid?, *J. Chem. Educ.* 1963, **40**(7), 379.

3. Sposito, G. *The Chemistry of Soils*; Sposito, G., Ed.; Oxford University Press: Oxford, 1989.

4. Hedges, J. I.; Prahl, F. G. Early Diagenesis: Consequences for application of molecular biomarkers, *Organic Geochemistry*; Engel, M. H., Ed: Plenum Press: New York, 1993.

5. Gaffney, J. S.; Marley, N. A.; Clark, S. B. Humic and fulvic acids and organic colloidal materials in the environment, *Humic and Fulvic Acids*; Gaffney, J. S.; Marley, N. A.; Clark, S. B., Ed.; American Chemical Society: Washington DC, 1996.

6. Sjostrom, E. *Wood Chemistry, 2nd ed.*; Academic Press: New York, 1993.

7. Schnitzer, M.; Oritz De Serra, M. I. The chemical degradation of a humic acid, *Can. J. Chem.* 1973, **51**, 1554.

8. Mycke, B.; Michaelis, W. Molecular fossils from chemical degradation of macromolecular organic matter, *Org. Geochem.* 1986, **10**, 847.

9. Schulten, H. R.; Schnitzer, M. A contribution to solving the puzzle of the chemical structure of humic substances, *Sci. Total. Environ.* 1992, **117**, 27.

10. Schulten, H. R.; Schnitzer, M. Temperature-resolved in source pyrolysis-soft ionization mass spectrometry of soil humic acids, *Org Geochem.* 1993, **2**, 17.

11. Bortiatynski, J. M.;Hatcher, P. G.; Knicker, H. NMR techniques in studies of humic substances, *Humic and Fulvic Acids*; Gaffney, J. S.; Marley, N. A.; Clark, S. B., Ed.; American Chemical Society: Washington DC, 1996.

12. Steelink, C. Application of liquid-state NMR spectroscopy to humic substances, *Humic Substances II*; Hayes, M. H. B., Ed ; Wiley Interscience: New York, 1989.

13. Wilson, M. A. Solid-state NMR spectroscopy of humic substances: basic concepts and techniques, *Humic Substances II*; Hayes, M. H. B., Ed; Wiley Interscience: New York, 1989.

14. Ricca, G.; Severini, F. Structural investigation of humic substances by IR-FT, ^{13}C-NMR spectroscopy and comparison with a maleic oligomer of known structure, *Geoderma*. 1993, **58**, 233.

15. Visser, S. A. Comparative study on the elementary composition of fulvic and humic acids of aquatic organic and from soils and microbial substrates, *Water. Res.* 1983, **17**(10), 1393.

16. Suffet, I. H.; MacCarthy, P. Aquatic humic substances and their influence on the fate and treatment of pollutants, *Aquatic Humic Substances*; Suffet, I. H; MacCartyy, P., Ed; American Chemical Society: Washington DC, 1989.

17. Patrick, H. G. Aliphatic structure of humic acids, *Org. Geochem.* 1981, **3**(48), 43.

18. Robert, L. C.; Cooper, H. L. Structural characterization of a fulvic acid and a humic acid using solid-state ramp-cp-mass ^{13}C nuclear magnetic resonance, *Environ. Sci. Tech.* 1998, **32**(5), 719.

19. Winchester, J. W.; Duce, R. A. The air-water interface: particulate matter exchange across the air-water interface, *Fate of Pollutants in the Air and Water Environments, Vol 1.*; Suffet, I. H., Ed; Wiley Interscience: New York, 1977.

20. Rice, J. A.; MacCarthy, P. Characterization of a stream sediment humin, *Aquatic Humic Substances*; Suffet, I. H; MacCarthy, P., Ed; American Chemical Society: Washington DC, 1989.

21. Schwarzenbach, R. P.; Gshwend, P. M.; Imboden, D. M. *Environmental Organic Chemistry*; John Wiley & Sons: New York, 1993.

22. Senesi, N. Binding mechanisms of pesticides to soil humic substances, *Sci. Total. Environ.* 1992, **123**, 63.

23. Senesi, N.; Testini, C. Adsorption of some nitrogenated herbicides by soil humic acids, *Soil. Sci.* 1980, **10**, 314.

24. Senesi, N., Testini, C. Theoretical aspects and experimental evidence of the capacity of humic substances to bind herbicides by charge-transfer mechanisms, *Chemosphere*. 1984, **13**, 461.

25. Parris, G. E. Covalent binding of aromatic amines to humates, *Environ. Sci. Tech.* 1980, **14**, 1099.

26. Chiou, C. T.; Peters, L. J.; Freed, V. H. A physical concept of soil-water equilibria for nonionic organic compounds, *Science.* 1979, **206**(16), 831.

27. Maqueda, C. A study of the interaction between chlordimeform and humic acid from a typic chromozevert soil, *Soil. Sci.* 1983, **22**, 167.

28. Landrum, P. F.; Reinhold, M.D.; Nihart, S.R; Eadie, B. J. Predicting the bioavailability of xenobiotics to pontoporeia hoyi in the presence of humic and fulvic materials and natural dissolved organic matter, *Environ. Tox. Chem.* 1985, **4**, 459.

29. Hassett, J. P.; Milicic, E. Determination of equilibrium and rate constants for binding of a polychlorinated biphenyl congener by dissolved humic substances, *Environ. Sci. Tech.* 1985, **19**(7), 638.

30. Wolcott, A. R.; Shin, Y. O.; Chodan, J. J. Adsorption of DDT by soils, soil fractions, and biological materials, *J. Agr. Food. Chem.* 1970, **18**(6), 1129.

31. Carter, C. W.; Suffet, I. H. Binding of DDT to dissolved humic materials, *Environ. Sci. Tech.* 1982, **16**(11), 735.

32. Chiou, C. T.; Malcolm, R.L.; Brinton, T. I.; Kile, D. E. Water solubility enhancement of some organic pollutants and pesticides by dissolved humic and fulvic acids, *Envoron. Sci. Tech.* 1986, **20**(5), 502.

33. Chiou, C. T.; Schmedding, D. W. Partitioning of organic compounds in octanol-water systems, *Environ. Sci. Tech.* 1982, **16**(1), 4.

34. Chiou, C. T.; Porter, P. E.; Schmedding, D. W. Partition equilibria of nonionic organic compounds between soil organic matter and water, *Environ. Sci. Tech.* 1983, **17**(4), 227.

35. Karickhoff, S. W. Semi-empirical estimation of sorption of hydrophobic pollutants on natural sediments and soils, *Chemosphere.* 1981, **10**(8), 833.

36. Spurlock, F. C.; Biggar, J. W. Thermodynamics of organic chemical partition in soils, *Environ. Sci. Tech.* 1994, **28**(6), 989.

37. Swift, R. S. J. Molecular weight and shape of humic acid from sedimentation and diffusion measurements on fractionated extracts, *Soil. Sci.* 1972, **23**(4), 394.

38. Chin, Y. P.; Weber, W. J. J. Estimating the effects of dispersed organic polymers on the sorption of contaminants by natural solids, *Envrion. Sci. Tech.* 1989, **23**(8), 978.

39. Atik, S. S.; Thomas, J. K. Transport of phtoproduced ions in water in oil macroemulsions: movement of ions from one water pool to another, *J. Am. Chem. Soc.* 1981, **103**, 3543.

40. Burns, S. E.; Hassett, J. P.; Rossi, M. V. Binding effects of humic-mediated photoreaction: intrahumic dechlorination of mirex in water, *Environ. Sci. Tech.* 1996, **30**(10), 2934.

41. Atik, S. S.; Singer, L. A. A comparison of approximate and exact statistical models for intramicellar fluorescence quenching, *Chem. Phy. Lett.*1979, **66**(2), 234.

42. Zepp, R. G. Photoproduction of hydrated electrons from natural organic solutes in aquatic environments, *Environ. Sci. Tech.* 1987, **21**(5), 485.

43. Yin, C.; Hassett, J. P. Fugacity and phase distribution of mirex in oswego river and lake ontario waters, *Chemosphere.* 1989, **19**(8), 1289.

44. Driscoll, M. S.; Hassett, J. P.; Fish, C. L. Extraction efficiencies of organochlorine compounds from niagara river water, *Environ. Sci. Tech.* 1991. **25**(8), 1432.

45. Mackay, D.; Shiu, W. Y.; Sutherland, R. P. Determination of air-water Henry's law constants for hydrophobic pollutants, *Environ. Sci. Tech.* 1979, **13**(3), 333.

46. Liss, P. S.; Slater, P. G. Flux of gases across the air-sea interface, *Nature.* 1974, **247**, 181.

47. Evans, H. E. The binding of three PCB congeners to dissolved organic carbon in freshwaters, *Chemosphere.* 1988, **17**(12), 2325.

48. Gshwend, P. M.; Wu, S. On the constancy of sediment-water partition coefficients of hydrophobic organic pollutants, *Environ. Sci. Tech.* 1985, **19**(11), 90.

49. McCarthy, J. F; Jimenez, B. D. Interactions between polycyclic aromatic hydrocarbons and dissolved humic material, *Environ. Sci. Tech.* 1985, **19**(11), 1072.

50. Pardue, J. H.; Masscheleyn, P. H.; DeLaune, R. D.; Patrick, W. H. Assimilation of Hydrophobic chlorinated organics in freshwater wetlands: sorption and sediment-water exchange, *Environ. Sci. Tech.* 1993, **27**(5), 875.

51. Gvirtzman, H.; Gorelick, S. M. The concept of in-situ vapor stripping for removing vocs from groundwater, *Trans. Porous. Media.* 1992, **8**, 7.

52. Beckett, R. Surface and colloid chemistry in natural waters and water treatment, *The Surface Chemistry of Humic Substances in Aquatic Systems*; Beckett. R., Ed; Plenum Press: New York, 1990.

53. Wan, J.; Tokunaga, K. Measuring partition coefficients of colloids at air-water interfaces, *Environ. Sci. Tech.* 1998, **32**(21), 3293.

54. Oliver, B. G. Desorption of chlorinated hydrocarbons from spiked and anthoropogenically contaminated sediments, *Chemosphere.* 1985, **14(**8), 1087.

55. Lara, R.; Ernst, W. Interaction between polychlorinated biphenyls and marine humic substances, *Chemospher.* 1989, **19**(8), 1655.

56. Landrum, P. F. Reverse-phase separation method for determining pollutant binding to aldrich humic acid and dissolved organic carbon of natural waters, *Environ. Sci. Tech.* 1984, **18**(3), 187.

57. Wijayaratne, R. D.; Means, J. C. Sorption of polycyclic aromatic hydrocarbons by natural estuarine colloids, *Mar. Environ. Res.* 1984, **11**(2), 77.

Appendix A

Raw Data

HCB K_{DOC}' Raw Data

Initial HCB Concentration (ug/L)	Gas Flow Rate (L/min)	Solution Volume (L)	T (^{0}C)	[DOC] (mg/L)	K_{DOC}' $^{\#}$	SD*
2.5	3.75	2	25.5	27.7	68362	5516
2.5	3.75	2	25.5	55.7	45273	7462
2.5	3.75	2	25.5	106	19721	1672
2.5	3.75	2	24.7	112	1891	274.0
2.5	3.75	2	24.1	112.2	21013	2500
4.0	0.50	2	23.5	117	9830	3681
2.5	3.75	2	25.2	117	3487	253.2
2.5	2.00	2	24.7	150	1387	384.1
10	2.00	2	22.9	365.7	2222	170.3
10	2.00	2	22.9	731.5	2569	357.4
2.5	2.00	2	25.2	1829	4647	439.5

*SD: Standard deviation for K_{DOC}
$^{\#}K_{DOC}'$ values from Equation 42

QCB K_{DOC}' Raw Data

Initial QCB Concentration (ug/L)	Gas Flow Rate (L/min)	Solution Volume (L)	T (^{0}C)	[DOC] (mg/L)	K_{DOC}' #	SD*
10	2	2	22.9	365.7	6525	324
10	2	2	22.9	731.5	4830	418
20	2	2	25.2	1829	1048	250
20	2	2	24.7	150	3092	119
20	2	2	24.7	49.4	257.0	10.6
10	0.5	2	23.5	117	1588	210
10	3.75	2	24.1	112.2	1067	47.6
15	3	2	25.3	213	861.7	36.8

*SD: Standard deviation for K_{DOC}
#K_{DOC}' values from Equation 42

TeCB K_{DOC}' Raw Data

Initial TeCB Concentration (ug/L)	Gas Flow Rate (L/min)	Solution Volume (L)	T (^{0}C)	[DOC] (mg/L)	K_{DOC}' [#]	SD*
153	2	2	24.7	49.4	14129	1188
80	3.75	2	24.1	112.2	5760	711.9
80	0.5	2	23.5	117	630.5	102.3
153	2	2	24.7	150	1813	162.8
15.3	2	2	22.9	365.7	418.4	23.36
154	2	2	25.5	704	448.8	21.34
154	3.5	1.5	25.5	708	237.0	8.458
154	1	1.5	25.5	708	-46.75	4.865
154	3.5	2	25.5	731	1390	186.7
15.3	2	2	22.9	731.5	496.6	21.67
154	2	2	25.5	759	2372	398.2
153	2	2	25.2	1829	604.5	27.24

*SD: Standard deviation for K_{DOC}
[#] K_{DOC}' values from Equation 42

TCB K_{DOC}' Raw Data

Initial TCB Concentration (ug/L)	Gas Flow Rate (L/min)	Solution Volume (L)	T (^{0}C)	[DOC] (mg/L)	K_{DOC}' #	SD*
330	2	2	24.7	49.4	5395	483.6
210	0.5	2	23.5	117	3121	460.2
330	2	2	24.7	150	1104	68.79
33	2	2	22.9	365.7	-616.5	28.55
33	2	2	22.9	731.5	-235.5	16.72
655	2	2	25.2	1647	-52.19	4.169
330	2	2	25.2	1829	-46.57	4.639

*SD: Standard deviation for K_{DOC}
#K_{DOC}' values from Equation 42

DCB K_{DOC}' Raw Data

Initial DCB Concentration (ug/L)	Gas Flow Rate (L/min)	Solution Volume (L)	T (^{0}C)	[DOC] (mg/L)	K_{DOC}' #	SD*
322	2	2	24.7	49.4	3259	173.5
193	0.5	2	23.5	117	-963.6	128.0
322	2	2	24.7	150	719.0	32.12
322	2	2	25.2	1829	210.6	10.14

*SD: Standard deviation for K_{DOC}
#K_{DOC}' values from Equation 42

BIBLIOGRAPHY

Atik, S. S.; Singer, L. A. A comparison of approximate and exact statistical models for intramicellar fluorescence quenching, *Chem. Phy. Lett.*1979, **66**(2), 234.

Atik, S. S.; Thomas, J. K. Transport of phtoproduced ions in water in oil macroemulsions: movement of ions from one water pool to another, *J. Am. Chem. Soc.* 1981, **103**, 3543.

Beckett, R. Surface and colloid chemistry in natural waters and water treatment, *The Surface Chemistry of Humic Substances in Aquatic Systems*; Beckett. R., Ed; Plenum Press: New York, 1990.

Boogs, S. J.; Levermore, D. G.; Seitz, M. G. Humic macromolecules in natural waters, *J. Macromol. Sci. Rev.* 1985, **25**(4), 599.

Bortiatynski, J. M.;Hatcher, P. G.; Knicker, H. NMR techniques in studies of humic substances, *Humic and Fulvic Acids*; Gaffney, J. S.; Marley, N. A.; Clark, S. B., Ed.; American Chemical Society: Washington DC, 1996.

Burns, S. E.; Hassett, J. P.; Rossi, M. V. Binding effects of humic-mediated photoreaction: intrahumic dechlorination of mirex in water, *Environ. Sci. Tech.* 1996, **30**(10), 2934.

Carter, C. W.; Suffet, I. H. Binding of DDT to dissolved humic materials, *Environ. Sci. Tech.* 1982, **16**(11), 735.

Chin, Y. P.; Weber, W. J. J. Estimating the effects of dispersed organic polymers on the sorption of contaminants by natural solids, *Envrion. Sci. Tech.* 1989, **23**(8), 978.

Chiou, C. T.; Malcolm, R.L.; Brinton, T. I.; Kile, D. E. Water solubility enhancement of some organic pollutants and pesticides by dissolved humic and fulvic acids, *Envoron. Sci. Tech.* 1986, **20**(5), 502.

Chiou, C. T.; Peters, L. J.; Freed, V. H. A physical concept of soil-water equilibria for nonionic organic compounds, *Science.* 1979, **206**(16), 831.

Chiou, C. T.; Porter, P. E.; Schmedding, D. W. Partition equilibria of nonionic organic compounds between soil organic matter and water, *Environ. Sci. Tech.* 1983, **17**(4), 227.

Chiou, C. T.; Schmedding, D. W. Partitioning of organic compounds in octanol-water systems, *Environ. Sci. Tech.* 1982, **16**(1), 4.

Cornelium, S. What is humic acid?, *J. Chem. Educ.* 1963, **40**(7), 379.

Driscoll, M. S.; Hassett, J. P.; Fish, C. L. Extraction efficiencies of organochlorine compounds from niagara river water, *Environ. Sci. Tech.* 1991. **25**(8), 1432.

Evans, H. E. The binding of three PCB congeners to dissolved organic carbon in freshwaters, *Chemosphere.* 1988, **17**(12), 2325.

Gaffney, J. S.; Marley, N. A.; Clark, S. B. Humic and fulvic acids and organic colloidal materials in the environment, *Humic and Fulvic Acids*; Gaffney, J. S.; Marley, N. A.; Clark, S. B., Ed.; American Chemical Society: Washington DC, 1996.

Gshwend, P. M.; Wu, S. On the constancy of sediment-water partition coefficients of hydrophobic organic pollutants, *Environ. Sci. Tech.* 1985, **19**(11), 90.

Gvirtzman, H.; Gorelick, S. M. The concept of in-situ vapor stripping for removing vocs from groundwater, *Trans. Porous. Media.* 1992, **8**, 7.

Hassett, J. P.; Milicic, E. Determination of equilibrium and rate constants for binding of a polychlorinated biphenyl congener by dissolved humic substances, *Environ. Sci. Tech.* 1985, **19**(7), 638.

Hedges, J. I.; Prahl, F. G. Early Diagenesis: Consequences for application of molecular biomarkers, *Organic Geochemistry*; Engel, M. H., Ed: Plenum Press: New York, 1993.

Karickhoff, S. W. Semi-empirical estimation of sorption of hydrophobic pollutants on natural sediments and soils, *Chemosphere.* 1981, **10**(8), 833.

Landrum, P. F. Reverse-phase separation method for determining pollutant binding to aldrich humic acid and dissolved organic carbon of natural waters, *Environ. Sci. Tech.* 1984, **18**(3), 187.

Landrum, P. F.; Reinhold, M.D.; Nihart, S.R; Eadie, B. J. Predicting the bioavailability of xenobiotics to pontoporeia hoyi in the presence of humic and fulvic materials and natural dissolved organic matter, *Environ. Tox. Chem.* 1985, **4**, 459.

Lara, R.; Ernst, W. Interaction between polychlorinated biphenyls and marine humic substances, *Chemospher.* 1989, **19**(8), 1655.

Liss, P. S.; Slater, P. G. Flux of gases across the air-sea interface, *Nature*. 1974, **247**, 181.

Mackay, D.; Shiu, W. Y.; Sutherland, R. P. Determination of air-water Henry's law constants for hydrophobic pollutants, *Environ. Sci. Tech.* 1979, **13**(3), 333.

Maqueda, C. A study of the interaction between chlordimeform and humic acid from a typic chromozevert soil, *Soil. Sci.* 1983, **22**, 167.

McCarthy, J. F; Jimenez, B. D. Interactions between polycyclic aromatic hydrocarbons and dissolved humic material, *Environ. Sci. Tech.* 1985, **19**(11), 1072.

Mycke, B.; Michaelis, W. Molecular fossils from chemical degradation of macromolecular organic matter, *Org. Geochem.* 1986, **10**, 847.

Oliver, B. G. Desorption of chlorinated hydrocarbons from spiked and anthoropogenically contaminated sediments, *Chemosphere*. 1985, **14(**8), 1087.

Pardue, J. H.; Masscheleyn, P. H.; DeLaune, R. D.; Patrick, W. H. Assimilation of Hydrophobic chlorinated organics in freshwater wetlands: sorption and sediment-water exchange, *Environ. Sci. Tech.* 1993, **27**(5), 875.

Parris, G. E. Covalent binding of aromatic amines to humates, *Environ. Sci. Tech.* 1980, **14**, 1099.

Patrick, H. G. Aliphatic structure of humic acids, *Org. Geochem.* 1981, **3**(48), 43.

Ricca, G.; Severini, F. Structural investigation of humic substances by IR-FT, ^{13}C-NMR spectroscopy and comparison with a maleic oligomer of known structure, *Geoderma*. 1993, **58**, 233.

Rice, J. A.; MacCarthy, P. Characterization of a stream sediment humin, *Aquatic Humic Substances*; Suffet, I. H; MacCarthy, P., Ed; American Chemical Society: Washington DC, 1989.

Robert, L. C.; Cooper, H. L. Structural characterization of a fulvic acid and a humic acid using solid-state ramp-cp-mass ^{13}C nuclear magnetic resonance, *Environ. Sci. Tech.* 1998, **32**(5), 719.

Schnitzer, M.; Oritz De Serra, M. I. The chemical degradation of a humic acid, *Can. J. Chem.* 1973, **51**, 1554.

Schulten, H. R.; Schnitzer, M. A contribution to solving the puzzle of the chemical structure of humic substances, *Sci. Total. Environ.* 1992, **117**, 27.

Schulten, H. R.; Schnitzer, M. Temperature-resolved in source pyrolysis-soft ionization mass spectrometry of soil humic acids, *Org Geochem.* 1993, **2**, 17.

Schwarzenbach, R. P.; Gshwend, P. M.; Imboden, D. M. *Environmental Organic Chemistry*; John Wiley & Sons: New York, 1993.

Senesi, N. Binding mechanisms of pesticides to soil humic substances, *Sci. Total. Environ.* 1992, **123**, 63.

Senesi, N.; Testini, C. Adsorption of some nitrogenated herbicides by soil humic acids, *Soil. Sci.* 1980, **10**, 314.

Senesi, N., Testini, C. Theoretical aspects and experimental evidence of the capacity of humic substances to bind herbicides by charge-transfer mechanisms, *Chemosphere*. 1984, **13**, 461.

Sjostrom, E. *Wood Chemistry, 2nd ed.*; Academic Press: New York, 1993.

Sposito, G. *The Chemistry of Soils*; Sposito, G., Ed.; Oxford University Press: Oxford, 1989.

Spurlock, F. C.; Biggar, J. W. Thermodynamics of organic chemical partition in soils, *Environ. Sci. Tech.* 1994, **28**(6), 989.

Steelink, C. Application of liquid-state NMR spectroscopy to humic substances, *Humic Substances II*; Hayes, M. H. B., Ed ; Wiley Interscience: New York, 1989.

Suffet, I. H.; MacCarthy, P. Aquatic humic substances and their influence on the fate and treatment of pollutants, *Aquatic Humic Substances*; Suffet, I. H; MacCartyy, P., Ed; American Chemical Society: Washington DC, 1989.

Swift, R. S. J. Molecular weight and shape of humic acid from sedimentation and diffusion measurements on fractionated extracts, *Soil. Sci.* 1972, **23**(4), 394.

Visser, S. A. Comparative study on the elementary composition of fulvic and humic acids of aquatic organic and from soils and microbial substrates, *Water. Res.* 1983, **17**(10), 1393.

Wan, J.; Tokunaga, K. Measuring partition coefficients of colloids at air-water interfaces, *Environ. Sci. Tech.* 1998, **32**(21), 3293.

Wijayaratne, R. D.; Means, J. C. Sorption of polycyclic aromatic hydrocarbons by natural estuarine colloids, *Mar. Environ. Res.* 1984, **11**(2), 77.

Wilson, M. A. Solid-state NMR spectroscopy of humic substances: basic concepts and techniques, *Humic Substances II*; Hayes, M. H. B., Ed; Wiley Interscience: New York, 1989.

Winchester, J. W.; Duce, R. A. The air-water interface: particulate matter exchange across the air-water interface, *Fate of Pollutants in the Air and Water Environments, Vol 1.*; Suffet, I. H., Ed; Wiley Interscience: New York, 1977.

Wolcott, A. R.; Shin, Y. O.; Chodan, J. J. Adsorption of DDT by soils, soil fractions, and biological materials, *J. Agr. Food. Chem.* 1970, **18**(6), 1129.

Yin, C.; Hassett, J. P. Fugacity and phase distribution of mirex in oswego river and lake ontario waters, *Chemosphere*. 1989, **19**(8), 1289.

Zepp, R. G. Photoproduction of hydrated electrons from natural organic solutes in aquatic environments, *Environ. Sci. Tech.* 1987, **21**(5), 485.